(19) Europäisches Patentamt
European Patent Office
Office européen des brevets

(11) Publication number: **0 578 836 A1**

(12) **EUROPEAN PATENT APPLICATION published in accordance with Art. 158(3) EPC**

(21) Application number: **93903324.7**

(51) Int. Cl.5: **H01S 3/18**, H01S 3/094

(22) Date of filing: **05.02.93**

(86) International application number:
**PCT/JP93/00156**

(87) International publication number:
**WO 93/16513 (19.08.93 93/20)**

(30) Priority: **05.02.92 JP 20289/92**

(43) Date of publication of application:
**19.01.94 Bulletin 94/03**

(84) Designated Contracting States:
**DE FR GB IT NL**

(71) Applicant: **MITSUI PETROCHEMICAL INDUSTRIES, LTD.**
**2-5, Kasumigaseki 3-chome**
**Chiyoda-ku**
**Tokyo 100(JP)**

(72) Inventor: **MURO, Kiyofumi Mitsui Petrochemical Industries, Ltd.**
**580-32, Aza-Taku 2-gou**
**Nagaura**
**Sodegaura-shi**
**Chiba 299-02(JP)**
Inventor: **FUJIMOTO, Tsuyoshi Mitsui Petrochemical Ind. Ltd.**
**580-32, Aza-Taku 2-gou**
**Nagaura**
**Sodegaura-shi**
**Chiba 299-02(JP)**
Inventor: **YOSHIDA, Yuuji Mitsui Petrochemical Industries, Ltd.**
**580-32, Aza-Taku 2-gou**
**Nagaura**
**Sodegaura-shi**
**Chiba 299-02(JP)**
Inventor: **YAMADA, Yoshikazu Mitsui Petrochemical Industries Ltd.**
**580-32, Aza-Taku 2-gou**
**Nagaura**
**Sodegaura-shi**
**Chiba 299-02(JP)**
Inventor: **ISHIZAKA, Shoji Mitsui Petrochemical Industries, Ltd.**
**580-32, Aza-Taku 2-gou**
**Nagaura**
**Sodegaura-shi**
**Chiba 299-02(JP)**

(74) Representative: **Lehn, Werner, Dipl.-Ing. et al**
**Hoffmann, Eitle & Partner, Patentanwälte,**
**Postfach 81 04 20**
**D-81904 München (DE)**

(54) **SEMICONDUCTOR LASER ELEMENT AND LASER MANUFACTURED USING THE SAME.**

(57) A semiconductor laser provided with barrier layers which are arranged on both cross sections of an active layer formed in the direction vertical to the surface of the device in order to weaken the light waveguide function of the active layer, waveguide layers having band gaps and arranged on both sides of the barrier layers, and clad layers sandwiching the waveguide layers. This structure overcomes the dilemma in designing a device for controlling the waveguide mode encountered in conventional weakly-guided lasers and LOC-structure lasers.

EP 0 578 836 A1

Moreover, problems such as of obtaining a higher output, a smaller divergence of the emitted beam, and an improvement of the beam profile are solved.

FIG.1(a)

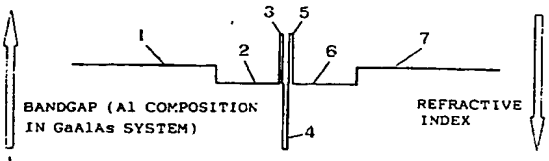


FIG.1(b)

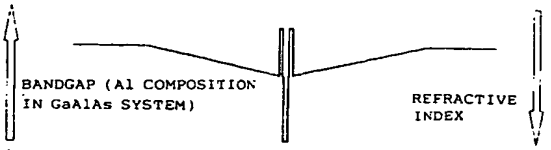


FIG.1(c)

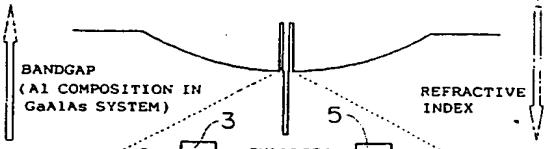


FIG.1(d)

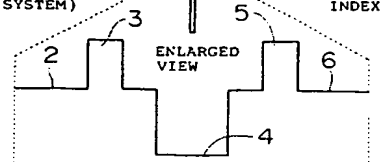


FIG.1(e)

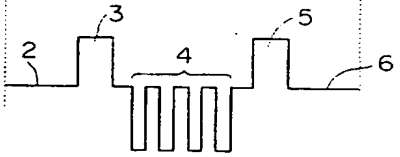

## Technical Field

The present invention relates generally to industrial fields in which high-output semiconductor lasers are employed for communications, optical recording on optical disks or the like, laser printers, laser medical treatments, laser machining, etc.. The present invention relates, more particularly, to a high-output semiconductor laser for a solid-state laser excitation requiring laser beams having an enhanced output and a small radiation angle or for a harmonic conversion element excitation and also to a laser device using this semiconductor laser.

## Background Arts

It has been desired in many sectors that the output of the semiconductor laser be enhanced. A factor for hindering the output enhancement per single mode of the semiconductor laser is a single surface fusion caused by the laser beam which is called a concurrent optical damage (COD). The COD is conspicuous especially in an AlGaAs system laser. Paying attention mainly to a reduction of a power density of the laser by expanding a laser guided mode, a weakly guiding laser having a thin active layer or a separate confinement type laser known as an LOC structure have hitherto been examined.

Based on such a structure, however, a strong correlation exists between a refractive index and a bandgap of each mixed crystal system in a variety of laser materials ranging from the AlGaAs system. It is therefore impossible to independently control a carrier confinement and an optical confinement in a waveguide.

In particular, the expansion of the guided mode requires the thin active layer in either the LOC structured laser or the weakly guiding laser for the output enhancement. Further, a wide active layer is needed for obtaining a high gain for oscillations in the expanded guided mode. A self-contradiction thus exists therein. As a matter of fact, a limit of the mode expansion in an epitaxial direction by the above-mentioned methods is approximately 1 $\mu$m at the maximum. A limit of the output thereof is on the order of 100 mW per single mode.

Besides, in the weakly guiding laser having the thin active layer, the guided mode in the laminated direction exhibits an exponential function profile like a gentle slope mountain. Hence, a radiation density in the active layer where the concurrent optical damage is caused is high as compared with the whole beam intensity. This is disadvantageous for the output enhancement. Besides, the guided mode has tails drawn deeply in the clad layers, and hence there is needed a growth of the clad layers that are considerably thick for the expansion of the guided mode.

In addition, both the guided mode (near-field pattern) and a beam radiation angle (far-field pattern) deviate largely from the Gaussian beam conceived as ideal one. There exists a problem in terms of a convergence of the beams in multiple applications.

On the other hand, there have been also examined lasers based on a so-called window structure in which the vicinity of a COD-induced outgoing single surface is made transparent to the laser emission beam and a structure where a carrier implantation is not effected in the vicinity of the signal surface. Those structures generally present, however, such problems that the astigmatism increases in addition to a complicated manufacturing process.

Further, there has been made an attempt to manufacture the high-output laser in the single mode by an optical feedback between a multiplicity of semiconductor lasers. The problem is, however, that the device becomes complicated.

It is an object of the present invention in view of the fact that multi-layered thin films have been easily formed by the molecular beam eitaxial (MBE) method, the metal organic chemical vapor deposition (MOCVD) method, etc. in recent years to solve the problems inherent in the conventional weakly guiding lasers and the LOC structured lasers in terms of overcoming the dilemma in designing the device for controlling the guided mode, attaining the output enhancement, the low dispersion of the radiation beams and improving the beam profile.

## Disclosure of Invention

According to the present invention, barrier layers having barrier heights enough to cancel a guiding characteristic of an active layer and perform a carrier confinement in the active layer are inserted on both sides of the active layer of an ordinary double hetero laser or a quantum well laser. It is therefore possible to perform the confinement in the guided mode and independently design an active layer thickness required for oscillations.

On this occasion, a guiding function of the active layer can be canceled by the barrier layer while reducing an area of the active layer and a thickness of this barrier layer by a factor of some number of the oscillation wavelength. Under such conditions, the wave guide layers are further formed, and clad layers having a small difference of refractive index are formed at both edges of the wave guide layer for the purpose of controlling only light guiding. Formed alternatively are wide wave guide layers based on a graded-index structure of a straight line, a quadratic curve, etc.. It is thus possible to design the guided mode completely independently of the active layer design parameters, thereby obtaining a stable mode approximate to the Gaussian beams and the radiation beams having the high output and low dispersion angle.

With the intention of enhancing the output of the semiconductor laser by avoiding the concurrent optical damage on the edge surface and of decreasing a divergence angle of the beam radiation, it is required that the guided mode be expanded by setting to so-called weakly guiding. The optical gain in the active layer, however, has a fixed limit as seen in the gain saturation of, e.g., the quantum well laser. For this reason, the wide active layer or one quantum well layer is inevitably required to be multi-layered for maintaining the oscillations in the expanded guided mode. This induces the self-contradiction with the weakly guiding structure and therefore causes a problem in terms of designing a laser diode having a high-output and a low radiation beam angle.

The number of the quantum wells and the thickness of the active layer for giving the necessary optical gain to the oscillations independently of the weakly guiding process can be set because of the existence of the barrier layers incorporating the anti-guiding function described above. Particularly, the guiding function of the active layer area is canceled by the anti-guiding function of the barrier layer. The design of the active layer is compatible with the design of the guided mode by further separately introducing, into the wave guide layer, a mechanism for controlling the guided mode exhibiting, as illustrated in FIGS. 1-(a), 1-(b) and 1-(c), a refractive index distribution of a stepped, straight line or quadratic curve. It is therefore feasible to obtain the stable characteristic approximate to the radiation beams having the high-output and low dispersion angle, i.e., the Gaussian beams.

The present invention can be readily actualized by use of the hyperthin semiconductor manufacturing equipment such as a molecular beam epitaxial (MBE) system, a metal organic chemical vapor deposition (MOCVD) system or a metal organic molecular beam epitaxial (MOMBE) system. Further, the effects of this invention are remarkable in the laser diode using AlGa As system semiconductors. Substantially the same effects can be, however, expected in a variety of III-V group semiconductor materials of a GaInAs system, an AlGaInAs system, a GaInAsP system and a AlGaInP system and further in various types of II-VI group semiconductor lasers.

As illustrated in FIG. 1, the thin film layers are interposed on both sides of the active layer of the laser based on the conventional double hetero type structure or a multiple quantum well structure. The thin film layers are composed of materials having a barrier height enough to effect a carrier confinement in the active layer, a smaller refractive index than that of the wave guide layer and a wide gap. The thin film layers also incorporate the function to cancel the guiding characteristic of the active layer, the anti-guiding function and the carrier block function.

Further, it is possible to reduce a resistance due to the formation of a Schottky barrier on a band discontinuous surface and perform effective carrier blocking by performing P-doping on the order of $10^{18}/cm^3$ on the P-side of the thin film layer and N-doping on the N-side.

The cancellation of the guiding function of the active layer area by the barrier layer having the anti-guiding function can be substantially attained when establishing the following relationship under such condition that a thickness of the both is reduced by a factor of some number of the oscillation wavelength.

$$d_0 \times (N_{12} - N_0^2)^{0.5} = 2 \times d_1 (N_0^2 - N_2^2)^{0.5}$$

where, as substantially shown in FIG. 1, $N_0$ is the refractive index of the wave guide layer, $N_1$, $d_0$ are respectively the refractive index and the thickness of the active layer, and $N_2$, $d_1$ are respectively the refractive index and the thickness of the barrier layer. If the active layer is multi-layered as seen in the multiple quantum well structure, a quantity corresponding to the left side is calculated with respect to each layer. An added value thereof may be employed for the left side. More specifically, in the case of the active layer composed of the m-layered quantum well having a thickness $d_w$ wherein a composition of the barrier layer between the quantum wells is the same as that of the wave guide layer, the guiding function of the active layer can be canceled by the barrier layer when establishing the following relationship:

$$m \times d_w \times (N_1^2 - N_0^2)^{0.5} = 2 \times d_1 (N_0^2 - N_2^2)^{0.5}$$

When the guiding function of the active layer is canceled by the barrier layer, the guided mode is independently controllable by clad layers and the wave guide layers provided therearound. It is desirable that a cut-off state be present with respect to a higher-order mode because of the signal mode oscillations in any of the structures shown in FIGS. 1-(a), 1-(b) and 1-(c). Speaking of a step index type guiding mechanism shown in FIG. 1-(a), this guided mode can be described by the normalized frequency V. The normalized frequency V is defined by the following formula:

$$V = (\pi d / \lambda) \times (N_0^2 - N_3^2)^{0.5}$$

where $\pi$ is the ratio of the circumference of a circle to its diameter, $\lambda$ is the oscillation wavelength (angstrom), d is the thickness (angstrom) of the wave guide layer including the active layer and the barrier layer, $N_0$ is the refractive index of the wave guide layer, and $N_3$ is the refractive index of the clad layer.

In a symmetric waveguide, the normalized frequency is $\pi/2$ or under, and single mode guiding is effected. Note that guided mode exhibits a profile of a sinusoidal function within the wave guide core layer but a profile of a exponential function within the clad layer. When $V = \pi / 2$, a mode confinement rate in the wave guide layer is approximately 65%. Unlike the profile of the exponentiat function over the substantially entire area of the conventional weakly guiding laser, the guided mode approximates the Gaussian type (see FIG. 2). The structures (shown in FIGS. 2 and 3, respectively) in the embodiments 1 and 2 are designed substantially under this condition.

In the approximate-to-symmetry guiding structure, there is almost no possibility in which an odd-order mode is excited. Hence, even when making the mode more approximate to the Gaussian type by further increasing the normalized frequency up to a level on the order of $\pi$, the same effects can be acquired without causing multiple transverse mode oscillations. The embodiment 3 having the structure shown in FIG. 4 gives a design example where V is approximate to $\pi$.

Further, the one-layered oscillation mode can be made approximate to the Gaussian type by adopting the graded-index structure as shown in FIGS. 1-(b) and 1-(c).

We have repeated a trial manufacture of the semiconductor laser on the basis of the above-mentioned as a guideline and could obtain the following conditions with respect to the barrier layer. $V_0$ is defined by:

$$V_0 = \pi \cdot d / \lambda \cdot (N_1^2 - N_0^2)^{0.5}$$

where $\pi$ is the ratio of the circumference of a circle to its diameter, d is the thickness of the active layer, $\lambda$ is the oscillation wavelength (angstrom), and $N_1$ is the refractive index of the wave guide layer. If the active layer consists of N-pieces of multiple quantum wells, $V_0$ is expressed such as:

$$V_0 = N \cdot \pi \cdot d / \lambda \cdot (N_1^2 - N_0^2)^{0.5}$$

where d is the thickness of the well layer, $N_1$ is the refractive index of the well layer, and $N_0$ is the refractive index of the wave guide layer.

Next, $V_1$ is defined such as:

$$V_1 = \pi \cdot d / \lambda \, (N_0^2 - N_2^2)^{0.5}$$

where $\pi$ is the ratio of the circumference of a circle to its diameter, d is the thickness of the barrier layer, $N_2$ is the refractive index of the barrier layer, and $N_0$ is the refractive index of the wave guide layer.

Next, $V_2$ is defined by:

$$V_2 = \pi \cdot d / \lambda \cdot (N_0^2 - N_3^2)^{0.5}$$

where $\pi$ is the ratio of the circumference of a circle to its diameter, d is the inter clad layer thickness, $N_0$ is the refractive index of the wave guide layer, and $N_3$ is the refractive index of the clad layer.

As obvious from the formulas described above, $V_0$, $V_1$, $V_2$ respectively correspond to the normalized frequencies of the active layer, the barrier layer and the wave guide layer. If the anti-guiding function of the barrier layer is too large, a reentrant is formed in the vicinity of the active layer in the guided mode. As a result, the optical confinement rate is decreased. This brings about an increment in the threshold current. Accordingly, an influence of the barrier layer on the guided mode has to be lessened. According to the present invention, a variety of trial manufactures of the semiconductor laser have been repeated. Con-

sequently, it was found out that the barrier layer exerts a trace of influence on the whole guided mode, where the following relationship is established:

$$V_1 < V_2 / 10$$

Moreover, it was also confirmed through the various trial manufactures of the semiconductor laser that especially the following condition is effective in canceling the guiding mode of the active layer by the barrier layer:

$$V_0 / 3 < V_1 < V_0$$

Furthermore, the barrier layer has to effectively confine the carrier in the active layer. We have found out that the carrier can be sufficiently effectively confined in the active layer when $E > 2.5 \times 10^3 / d^2$, where d (angstrom) is the thickness of the barrier layer, and E (eV) is the energy gap difference between the wave guide layer and the barrier layer.

Herein, the composition of the wave guide layer is set preferably to $Al_xGa_{1-x}As$ ($0 \leq x < 0.35$: where x is the atomic ratio) in the semiconductor laser using $Al_xGa_{1-x}As$ ($0 \leq x < 1$). Further, when the composition of the wave guide layer is $Al_xGa_{1-x}As$ (however $0 \leq x < 1$), the relationship between x and the thickness d (angstrom) of the barrier layer preferably falls within the following range:

$$x > (2.2 \times 10^3 / d^2), \text{ and } x < (5.0 \times 10^4 / d^2O)$$

Further, $V_0$ is given by:

$$V_0 = \pi \cdot d_0 / \lambda \cdot (N_1^2 - N_0^2)^{0.5}$$

where $d_0$ is the thickness of the active layer. If the active layer consists of N-pieces of quantum well layers, however, $V_0$ is defined by:

$$V_0 = N \cdot \pi \cdot d_0 / \lambda \cdot (N_1^2 - N_0^2)^{0.5}$$

where $d_0$ is the thickness of the quantum well layer, $N_1$ is the refractive index of the quantum well layer, and $N_0$ is the refractive index of the wave guide layer. Then, a relationship therebetween is set preferably as follows:

$$(V_0 / 3) < V_1 < V_0$$

The barrier layers has a large bandgap on both sides of the active layer but a small refractive index and incorporates an anti-guiding function. These barrier layers act to reduce or cancel the guiding function incorporated into the active layer. Another function thereof is to block the implanted carriers and acts to confine the electrons and holes in the active layer. This layer also undergoes P- or N-doping , thereby ameliorating the resistance reducing function or the carrier confinement function.

The guided mode control structure of the wave guide layer provides the action to control the expansion of the oscillation mode and the profile with a stability as well.

## Brief Description of Drawings

[FIG. 1]

FIG. 1 is a schematic sectional view of a composition of a semiconductor laser in an epitaxial direction according to the invention.

[FIG. 2]

FIG. 2 is a schematic sectional view of a composition in an embodiment 1 of this invention.

[FIG. 3]

FIG. 3 is a schematic sectional view of a composition in an embodiment 2 of this invention.

[FIG. 4]

FIG. 4 is a schematic sectional view of a composition in an embodiment 3 of this invention.

[FIG. 5]

FIG. 5 is a schematic sectional view of a composition in an embodiment 4 of this invention. [FIG. 6]

FIG. 6 is a schematic sectional view of a composition in an embodiment 5 of this invention.

[FIG. 7]

FIG. 7 is a schematic sectional view of a composition in an embodiment 6 of this invention.

[FIG. 8]

FIG. 8 is a schematic sectional view of a composition in an embodiment 7 of this invention.

[FIG. 9]

FIG. 9 is a schematic sectional view of a composition in an embodiment 8 of this invention.

[FIG. 10]

FIG. 10 is a schematic sectional view of a composition in an embodiment 9 of this invention.

[FIG. 11]

FIG. 11 is a schematic sectional view of a composition in an embodiment 10 of this invention.

[FIG. 12]

FIG. 12 is a schematic sectional view of a composition in an embodiment 11 of this invention.

[FIG. 13]

FIG. 13 is a schematic sectional view of a composition in an embodiment 12 of this invention.

[FIG. 14]

FIG. 14 is a schematic sectional view of a composition in an embodiment 13 of this invention.

[FIG. 15]

FIG. 15 is a schematic sectional view of a composition in an embodiment 14 of this invention.

[FIG. 16]

FIG. 16 is a schematic sectional view of a composition in an embodiment 15 of this invention.

[FIG. 17]

FIG. 17 is a schematic sectional view of a composition in an embodiment 16 of this invention.

[FIG. 18]

FIG. 18 is a schematic sectional view of a composition in an embodiment 17 of this invention.

[FIG. 19]

FIG. 19 is a schematic sectional view of a composition in an embodiment 18 of this invention.

[FIG. 20]

FIG. 20 is a schematic sectional view of a composition in a comparative example in relation to the present invention.

[FIG. 21]

FIG. 21 is a graphic chart showing guided mode characteristics in the embodiments 1 ~ 3 and a reference example.

[FIG. 22]

FIG. 22 is a graphic chart showing characteristics of a radiation beam angle in the embodiments 1 ~ 3 and the reference example.

[FIG. 23]

FIG. 23 is a graphic chart showing the guided mode characteristics in embodiments 4 ~ 7.

[FIG. 24]

FIG. 24 is a graphic chart showing the characteristics of the radiation beam angle in the embodiments 4 ~ 7.

[FIG. 25]

FIG. 25 is a graphic chart showing the guided mode characteristics in embodiments 1 and 8 ~ 10.

[FIG. 26]

FIG. 26 is a graphic chart showing the characteristics of the radiation beam angle in the embodiments 1 and 8 ~ 10.

[FIG. 27]

FIG. 27 is a graphic chart showing the guided mode characteristics in embodiments 11 ~ 14.

[FIG. 28]

FIG. 28 is a graphic chart showing the characteristics of the radiation beam angle in the embodiments 11 ~ 14.

[FIG. 29]

FIG. 29 is a graphic chart showing the guided mode characteristics in embodiments 15 ~ 18.

[FIG. 30]

FIG. 30 is a graphic chart showing the characteristics of the radiation beam angle in the embodiments 15 ~ 18.

[FIG. 31]

FIG. 31 is a graphic chart representing an effective range of a barrier layer.

[FIG. 32]

FIG. 32 is a view illustrating a direct-connection type semiconductor laser excitation solid-state laser device utilizing the laser element according to this invention.

[FIG. 33]

FIG. 33 is a view illustrating an example of a fiber connection type semiconductor laser excitation solid-state laser device utilizing the laser element according to this invention.

## Best Mode For Carrying Out The Invention

The present invention will hereinafter be described on the basis of the drawings.

Epitaxial growths exhibiting profiles illustrated in FIGS. 2 ~ 20 are performed by MOCVD semiconductor thin film manufacturing equipment. FIG. 2 shows an embodiment 1. FIG. 3 shows an embodiment 2. FIG. 4 shows an embodiment 3. FIG. 5 shows an embodiment 4. FIG. 6 shows an embodiment 5. FIG. 7 shows an embodiment 6. FIG. 8 shows an embodiment 7. FIG. 9 shows an embodiment 8. FIG. 10 shows an embodiment 9. FIG. 11 shows an embodiment 10. FIG. 12 shows an embodiment 11. FIG. 13 shows an embodiment 12. FIG. 14 shows an embodiment 13. FIG. 15 shows an embodiment 14. FIG. 16 shows in an embodiment 15. FIG. 17 shows an embodiment 16. FIG. 18 shows an embodiment 17. FIG. 19 shows an embodiment 18. FIG. 20 is a schematic plan view thereof in a comparative example. FIG. 21 is a graphic chart showing a guided mode in the embodiments 1 ~ 3 and the comparative example. FIG. 22 is a graphic chart showing a radiation mode in the embodiments 1 ~ 3 and the comparative example. FIG. 23 is a graphic chart showing a guided mode in the embodiments 4 ~ 7. FIG. 24 is a graphic chart showing a radiation mode in the embodiment 4 ~ 7. FIG. 25 is a graphic chart showing a guided mode in the embodiments 1 and 8 ~ 10. FIG. 26 is a graphic chart showing a radiation mode in the embodiments 1 and 8 ~ 10. FIG. 27 is a graphic chart showing a guided mode in the embodiments 11 ~ 14. FIG. 28 is a graphic chart showing a radiation mode in the embodiments 11 ~ 14. FIG. 29 is a graphic chart showing a guided mode in the embodiments 15 ~ 18. FIG. 30 is a graphic chart showing a radiation mode in the embodiments 15 ~ 18. FIG. 31 is a graphic chart representing an effective range of a barrier layer, wherein the axis of abscissa indicates a difference in Al composition, and the axis of ordinate indicates a width of the barrier layer.

In FIG. 31, the anti-guiding function of the barrier layer is too large enough to exert a great influence on the guided mode in an upper range from the right upper curve. Concretely, a reentrant is formed in the guided mode in the vicinity of the active layer. This brings about a decrease in the optical confinement rate, resulting in an increment in threshold current. Further, it follows that the guided mode deviates largely from the Gaussian type, and an aberration is caused in the radiation pattern. The carrier confinement is insufficient enough to worsen a temperature characteristic of the threshold current in a lower range from the left lower curve. The guiding function of the active layer is compensated most optimally by the barrier layer to exhibit the best guided mode in a range where the following relationship is established:

$$V_0 / 3 < V_1 < V_0$$

The embodiments falling within this range are marked with ◎. (1) Represents the embodiment 1, and (2) indicates the embodiment 2. The circled numerals in the same Figure (FIG. 31) hereinafter similarly represent the embodiments corresponding to the numerals.

An effective range (exhibiting the effects) in the present invention is defined by the two solid lines.

The following is a technology common to the respective embodiment. Doping on the order of $1 \times 10^{18}/cm^3$ is conducted by use of Se as an n-type dopant and Zn as a p-type dopant. Zinc is diffused in a striped shape from the surface by use of an $SiO_2$ diffusion mask. Thereafter, a trail manufacture of a diode chip having a gain guiding structure is conducted by effecting a cleavage. After performing die-bonding to an LD mount, an oscillation characteristic is measured in a pulse mode. Table 1 shows characteristic of the typical chip having s stripe width of 2,5 μm and a cavity length of 300 μm. Note that no optical coating is applied to both edge surfaces.

(Embodiment 1)

As illustrated in FIG. 2, an n-type buffer layer 10 having a thickness of 0.5 μm is formed on an n-type substrate 8 composed of GaAs. Formed sequentially on this layer are an n-type clad layer 1, an n-type light wave guide layer 2, an n-type barrier layer 3, an active layer 4, a p-type barrier layer 5, a p-type light wave guide layer 6 and a p-type clad layer 7. An n-type cap layer 11 is formed as an uppermost layer thereon.

The following are concrete configurations of the respective layers.

n-type cap layer 11
Thickness: 0.3 μm
Composition: GaAs

p-type clad layer 7
Thickness: 1.0 μm
Composition: $Al_{0.35}Ga_{0.65}As$

p-type light wave guide layer 6
Thickness: 0.46 μm
Composition: $Al_{0.30}Ga_{0.70}As$

n-type light wave guide layer 2
Thickness: 0.46 μm
Composition: $Al_{0.30}Ga_{0.70}As$

n-type clad layer 1
Thickness: 1.0 μm
Composition: $Al_{0.35}Ga_{0.65}As$

n-type buffer layer 10
Thickness: 0.5 μm
Composition: GaAs

n-type substrate 8
Composition: (100) GaAs

The active layer 4 is formed such that 4-layered quantum well layers 13 are each partitioned by barrier layers 14 between side barrier layers 12 deposited on inner walls of the respective barrier layers 5, 3 in an area sandwiched in between the p-type barrier layer 5 and the n-type barrier layer 3. The concrete configurations of this active layer 4 are given as follows:

p-type barrier layer 5
Thickness: 165 angstrom
Composition: $Al_{0.38}Ga_{0.62}As$

Side barrier layer 12
Thickness: 25 angstrom
Composition: $Al_{0.30}Ga_{0.70}As$

Quantum well layer 13
Thickness: 55 angstrom
Composition: GaAs

Barrier layer 14
Thickness: 50 angstrom
Composition: $Al_{0.30}Ga_{0.70}As$

n-type barrier layer 3
Thickness: 165 angstrom
Composition: $Al_{0.38}Ga_{0.62}As$

FIG. 21 illustrates a guided mode profile (near-field patterns) in the direction vertical to the epitaxy layer with respect to the structure shown in this embodiment. FIG. 22 shows a measured result in the radiation mode.

(Embodiment 2)

As illustrated in FIG. 3, the n-type buffer layer 10 having a thickness of 0.5 μm is formed on the n-type substrate 8 composed of GaAs. Formed sequentially on this layer are the n-type clad layer 1, the n-type light wave guide layer 2, the n-type barrier layer 3, the active layer 4, the p-type barrier layer 5, the p-type light wave guide layer 6 and the p-type clad layer 7. The n-type cap layer 11 is formed as an uppermost layer thereon.

The following are concrete configurations of the respective layers.

n-type cap layer 11
Thickness: 0.3 μm
Composition: GaAs

p-type clad layer 7
Thickness: 2.0 μm
Composition: $Al_{0.31}Ga_{0.69}As$

p-type light wave guide layer 6
Thickness: 0.93 μm
Composition: $Al_{0.30}Ga_{0.70}As$
n-type light wave guide layer 2
Thickness: 0.93 μm
Composition: $Al_{0.30}Ga_{0.70}As$
n-type clad layer 1
Thickness: 2.0 μm
Composition: $Al_{0.31}Ga_{0.69}As$
n-type buffer layer 10
Thickness: 0.5 μm
Composition: GaAs
n-type substrate 8
Composition: (100) GaAs

The active layer 4 is formed such that 8-layered quantum well layers 13 are each partitioned by the barrier layers 14 between the side barrier layers 12 deposited on the inner walls of the respective barrier layers 5, 3 in the area sandwiched in between the p-type barrier layer 5 and the n-type barrier layer 3. The concrete configurations of this active layer 4 are given as follows:

p-type barrier layer 5
Thickness: 330 angstrom
Composition: $Al_{0.50}Ga_{0.50}As$
Side barrier layer 12
Thickness: 25 angstrom
Composition: $Al_{0.30}Ga_{0.70}As$
Quantum well layer 13
Thickness: 55 angstrom
Composition: GaAs
Barrier layer 14
Thickness: 50 angstrom
Composition: $Al_{0.30}Ga_{0.70}As$
n-type barrier layer 3
Thickness: 330 angstrom
Composition: $Al_{0.30}Ga_{0.70}As$

FIG. 21 illustrates a guided mode profile (near-field pattern) in the direction vertical to the epitaxy layer with respect to the structure shown in this embodiment. FIG. 22 shows a measured result in the radiation mode.

(Embodiment 3)

As illustrated in FIG. 4, an n-type inversion layer 15 is provided between the p-type clad layer 7 and the p-type light wave guide layer 6. With the placement of this n-type inversion layer, the current can be narrowed down in the lateral direction in the vicinity of the active layer 4.

Namely, the light is confined also in the lateral direction owing to the n-type inversion layer 15, thereby making it possible to attain a stabilized off-axial mode. n-type cap layer 11
Thickness: 0.3 μm
Composition: GaAs
p-type clad layer 7
Thickness: 0.8 μm
Composition: $Al_{0.35}Ga_{0.65}As$
n-type inversion layer 15
Thickness: 0.2 μm
Composition: $Al_{0.35}Ga_{0.65}As$
p-type light wave guide layer 6
Thickness: 0.93 μm
Composition: $Al_{0.30}Ga_{0.70}As$
n-type light wave guide layer 2
Thickness: 0.93 μm
Composition: $Al_{0.30}Ga_{0.70}As$

n-type clad layer 1
Thickness: 1.0 μm
Composition: $Al_{0.35}Ga_{0.65}As$
n-type buffer layer 10
Thickness: 0.5 μm
Composition: GaAs
n-type substrate 8
Composition: (100) GaAs

The active layer 4 is formed such that the 8-layered quantum well layers 13 are each partitioned by the barrier layers 14 between the side barrier layers 12 deposited on the inner walls of the respective barrier layers 5, 3 in the area sandwiched in between the p-type barrier layer 5 and the n-type barrier layer 3. The concrete configurations of this active layer 4 are given as follows:

p-type barrier layer 5
Thickness: 330 angstrom
Composition: $Al_{0.50}Ga_{0.50}As$
Side barrier layer 12
Thickness: 25 angstrom
Composition: $Al_{0.30}Ga_{0.70}As$
Quantum well layer 13
Thickness: 55 angstrom
Composition: GaAs
Barrier layer 14
Thickness: 50 angstrom
Composition: $Al_{0.30}Ga_{0.70}As$
n-type barrier layer 3
Thickness: 330 angstrom
Composition: $Al_{0.50}Ga_{0.50}As$

FIG. 21 illustrates a guided mode profile (near-field pattern) in the direction vertical to the epitaxy layer with respect to the structure shown in this embodiment. FIG. 22 shows a measured result in the radiation mode.

(Embodiment 4)

As illustrated in FIG. 5, the n-type buffer layer 10 having a thickness of 0.5 μm is formed on the n-type substrate 8 composed of GaAs. Formed sequentially on this layer are the n-type clad layer 1, the n-type light wave guide layer 2, the n-type barrier layer 3, the active layer 4, the p-type barrier layer 5, the p-type light wave guide layer 6 and the p-type clad layer 7. The n-type cap layer 11 is formed as an uppermost layer thereon.

The following are concrete configurations of the respective layers.

n-type cap layer 11
Thickness: 0.3 μm
Composition: GaAs
p-type clad layer 7
Thickness: 1.0 μm
Composition: $Al_{0.35}Ga_{0.65}As$
p-type light wave guide layer 6
Thickness: 0.46 μm
Composition: $Al_{0.30}Ga_{0.70}As$
n-type light wave guide layer 2
Thickness: 0.46 μm
Composition: $Al_{0.30}Ga_{0.70}As$
n-type clad layer 1
Thickness: 1.0 μm
Composition: $Al_{0.35}Ga_{0.65}As$
n-type buffer layer 10
Thickness: 0.5 μm
Composition: GaAs
n-type substrate 8

Composition: (100) GaAs

The active layer 4 is formed such that the 4-layered quantum well layers 13 are each partitioned by the barrier layers 14 between the side barrier layers 12 deposited on the inner walls of the respective barrier layers 5, 3 in the area sandwiched in between the p-type barrier layer 5 and the n-type barrier layer 3. The concrete configurations of this active layer 4 are given as follows:

p-type barrier layer 5

Thickness: 100 angstrom

Composition: $Al_{0.38}Ga_{0.62}As$

Side barrier layer 12

Thickness: 25 angstrom

Composition: $Al_{0.30}Ga_{0.70}As$

Quantum well layer 13

Thickness: 55 angstrom

Composition: GaAs

Barrier layer 14

Thickness: 50 angstrom

Composition: $Al_{0.30}Ga_{0.70}As$

n-type barrier layer 3

Thickness: 100 angstrom

Composition: $Al_{0.38}Ga_{0.62}As$

FIG. 23 illustrates a guided mode profile (near-field pattern) in the direction vertical to the epitaxy layer with respect to the structure shown in this embodiment. FIG. 24 shows a measured result in the radiation mode.

(Embodiment 5)

As illustrated in FIG. 6, the n-type buffer layer 10 having a thickness of 0.5 μm is formed on the n-type substrate 8 composed of GaAs. Formed sequentially on this layer are the n-type clad layer 1, the n-type light wave guide layer 2, the n-type barrier layer 3, the active layer 4, the p-type barrier layer 5, the p-type light wave guide layer 6 and the p-type clad layer 7. The n-type cap layer 11 is formed as an uppermost layer thereon.

The following are concrete configurations of the respective layers.

n-type cap layer 11

Thickness: 0.3 μm

Composition: GaAs

p-type clad layer 7

Thickness: 1.0 μm

Composition: $Al_{0.35}Ga_{0.65}As$

p-type light wave guide layer 6

Thickness: 0.46 μm

Composition: $Al_{0.30}Ga_{0.70}As$

n-type light wave guide layer 2

Thickness: 0.46 μm

Composition: $Al_{0.30}Ga_{0.70}As$

n-type clad layer 1

Thickness: 1.0 μm

Composition: $Al_{0.35}Ga_{0.65}As$

n-type buffer layer 10

Thickness: 0.5 μm

Composition: GaAs

n-type substrate 8

Composition: (100) GaAs

The active layer 4 is formed such that the 4-layered quantum well layers 13 are each partitioned by the barrier layers 14 between the side barrier layers 12 deposited on the inner walls of the respective barrier layers 5, 3 in the area sandwiched in between the p-type barrier layer 5 and the n-type barrier layer 3. The concrete configurations of this active layer 4 are given as follows:

p-type barrier layer 5

Thickness: 200 angstrom

Composition: $Al_{0.38}Ga_{0.62}As$
Side barrier layer 12
Thickness: 25 angstrom
Composition: $Al_{0.30}Ga_{0.70}As$
Quantum well layer 13
Thickness: 55 angstrom
Composition: GaAs
Barrier layer 14
Thickness: 50 angstrom
Composition: $Al_{0.30}Ga_{0.70}As$
n-type barrier layer 3
Thickness: 200 angstrom
Composition: $Al_{0.38}Ga_{0.62}As$

FIG. 23 illustrates a guided mode profile (near-field pattern) in the direction vertical to the epitaxy layer with respect to the structure shown in this embodiment. FIG. 24 shows a measured result in the radiation mode.

(Embodiment 6)

As illustrated in FIG. 7, the n-type buffer layer 10 having a thickness of 0.5 μm is formed on the n-type substrate 8 composed of GaAs. Formed sequentially on this layer are the n-type clad layer 1, the n-type light wave guide layer 2, the n-type barrier layer 3, the active layer 4, the p-type barrier layer 5, the p-type light wave guide layer 6 and the p-type clad layer 7. The n-type cap layer 11 is formed as an uppermost layer thereon.

The following are concrete configurations of the respective layers.

n-type cap layer 11
Thickness: 0.3 μm
Composition: GaAs
p-type clad layer 7
Thickness: 1.0 μm
Composition: $Al_{0.35}Ga_{0.65}As$
p-type light wave guide layer 6
Thickness: 0.46 μm
Composition: $Al_{0.30}Ga_{0.70}As$
n-type light wave guide layer 2
Thickness: 0.46 μm
Composition: $Al_{0.30}Ga_{0.70}As$
n-type clad layer 1
Thickness: 1.0 μm
Composition: $Al_{0.35}Ga_{0.65}As$
n-type buffer layer 10
Thickness: 0.5 μm
Composition: GaAs
n-type substrate 8
Composition: (100) GaAs

The active layer 4 is formed such that the 4-layered quantum well layers 13 are each partitioned by the barrier layers 14 between the side barrier layers 12 deposited on the inner walls of the respective barrier layers 5, 3 in the area sandwiched in between the p-type barrier layer 5 and the n-type barrier layer 3. The concrete configurations of this active layer 4 are given as follows:

p-type barrier layer 5
Thickness: 330 angstrom
Composition: $Al_{0.38}Ga_{0.62}As$
Side barrier layer 12
Thickness: 25 angstrom
Composition: $Al_{0.30}Ga_{0.70}As$
Quantum well layer 13
Thickness: 55 angstrom
Composition: GaAs

Barrier layer 14
Thickness: 50 angstrom
Composition: $Al_{0.30}Ga_{0.70}As$
n-type barrier layer 3
Thickness: 330 angstrom
Composition: $Al_{0.38}Ga_{0.62}As$

FIG. 23 illustrates a guided mode profile (near-field pattern) in the direction vertical to the epitaxy layer with respect to the structure shown in this embodiment. FIG. 24 shows a measured result in the radiation mode.

(Embodiment 7)

As illustrated in FIG. 8, the n-type buffer layer 10 having a thickness of 0.5 μm is formed on the n-type substrate 8 composed of GaAs. Formed sequentially on this layer are the n-type clad layer 1, the n-type light wave guide layer 2, the n-type barrier layer 3, the active layer 4, the p-type barrier layer 5, the p-type light wave guide layer 6 and the p-type clad layer 7. The n-type cap layer 11 is formed as an uppermost layer thereon.

The following are concrete configurations of the respective layers.

n-type cap layer 11
Thickness: 0.3 μm
Composition: GaAs
p-type clad layer 7
Thickness: 1.0 μm
Composition: $Al_{0.35}Ga_{0.65}As$
p-type light wave guide layer 6
Thickness: 0.46 μm
Composition: $Al_{0.30}Ga_{0.70}As$
n-type light wave guide layer 2
Thickness: 0.46 μm
Composition: $Al_{0.30}Ga_{0.70}As$
n-type clad layer 1
Thickness: 1.0 μm
Composition: $Al_{0.35}Ga_{0.65}As$
n-type buffer layer 10
Thickness: 0.5 μm
Composition: GaAs
n-type substrate 8
Composition: (100) GaAs

The active layer 4 is formed such that the 4-layered quantum well layers 13 are each partitioned by the barrier layers 14 between the side barrier layers 12 deposited on the inner walls of the respective barrier layers 5, 3 in the area sandwiched in between the p-type barrier layer 5 and the n-type barrier layer 3. The concrete configurations of this active layer 4 are given as follows:

p-type barrier layer 5
Thickness: 500 angstrom
Composition: $Al_{0.38}Ga_{0.62}As$
Side barrier layer 12
Thickness: 25 angstrom
Composition: $Al_{0.30}Ga_{0.70}As$
Quantum well layer 13
Thickness: 55 angstrom
Composition: GaAs
Barrier layer 14
Thickness: 50 angstrom
Composition: $Al_{0.30}Ga_{0.70}As$
n-type barrier layer 3
Thickness: 500 angstrom
Composition: $Al_{0.38}Ga_{0.62}As$

FIG. 23 illustrates a guided mode profile (near-field pattern) in the direction vertical to the epitaxy layer

with respect to the structure shown in this embodiment. FIG. 24 shows a measured result in the radiation mode.

(Embodiment 8)

As illustrated in FIG. 9, the n-type buffer layer 10 having a thickness of 0.5 μm is formed on the n-type substrate 8 composed of GaAs. Formed sequentially on this layer are the n-type clad layer 1, the n-type light wave guide layer 2, the n-type barrier layer 3, the active layer 4, the p-type barrier layer 5, the p-type light wave guide layer 6 and the p-type clad layer 7. The n-type cap layer 11 is formed as an uppermost layer thereon.

The following are concrete configurations of the respective layers.

n-type cap layer 11
- Thickness: 0.3 μm
- Composition: GaAs

p-type clad layer 7
- Thickness: 1.0 μm
- Composition: $Al_{0.35}Ga_{0.65}As$

p-type light wave guide layer 6
- Thickness: 0.46 μm
- Composition: $Al_{0.30}Ga_{0.70}As$

n-type light wave guide layer 2
- Thickness: 0.46 μm
- Composition: $Al_{0.30}Ga_{0.70}As$

n-type clad layer 1
- Thickness: 1.0 μm
- Composition: $Al_{0.35}Ga_{0.65}As$

n-type buffer layer 10
- Thickness: 0.5 μm
- Composition: GaAs

n-type substrate 8
- Composition: (100) GaAs

The active layer 4 is formed such that the 4-layered quantum well layers 13 are each partitioned by the barrier layers 14 between the side barrier layers 12 deposited on the inner walls of the respective barrier layers 5, 3 in the area sandwiched in between the p-type barrier layer 5 and the n-type barrier layer 3. The concrete configurations of this active layer 4 are given as follows:

p-type barrier layer 5
- Thickness: 50 angstrom
- Composition: $Al_{0.50}Ga_{0.50}As$

Side barrier layer 12
- Thickness: 25 angstrom
- Composition: $Al_{0.30}Ga_{0.70}As$

Quantum well layer 13
- Thickness: 55 angstrom
- Composition: GaAs

Barrier layer 14
- Thickness: 50 angstrom
- Composition: $Al_{0.30}Ga_{0.70}As$

n-type barrier layer 3
- Thickness: 50 angstrom
- Composition: $Al_{0.30}Ga_{0.70}As$

FIG. 25 illustrates a guided mode profile (near-field pattern) in the direction vertical to the epitaxy layer with respect to the structure shown in this embodiment. FIG. 26 shows a measured result in the radiation mode.

(Embodiment 9)

As illustrated in FIG. 10, the n-type buffer layer 10 having a thickness of 0.5 μm is formed on the n-type substrate 8 composed of GaAs. Formed sequentially on this layer are the n-type clad layer 1, the n-type

light wave guide layer 2, the n-type barrier layer 3, the active layer 4, the p-type barrier layer 5, the p-type light wave guide layer 6 and the p-type clad layer 7. The n-type cap layer 11 is formed as an uppermost layer thereon.

The following are concrete configurations of the respective layers.

n-type cap layer 11
Thickness: 0.3 μm
Composition: GaAs
p-type clad layer 7
Thickness: 1.0 μm
Composition: $Al_{0.35}Ga_{0.65}As$
p-type light wave guide layer 6
Thickness: 0.46 μm
Composition: $Al_{0.30}Ga_{0.70}As$
n-type light wave guide layer 2
Thickness: 0.46 μm
Composition: $Al_{0.30}Ga_{0.70}As$
n-type clad layer 1
Thickness: 1.0 μm
Composition: $Al_{0.35}Ga_{0.65}As$
n-type buffer layer 10
Thickness: 0.5 μm
Composition: GaAs
n-type substrate 8
Composition: (100) GaAs

The active layer 4 is formed such that the 4-layered quantum well layers 13 are each partitioned by the barrier layers 14 between the side barrier layers 12 deposited on the inner walls of the respective barrier layers 5, 3 in the area sandwiched in between the p-type barrier layer 5 and the n-type barrier layer 3. The concrete configurations of this active layer 4 are given as follows:

p-type barrier layer 5
Thickness: 330 angstrom
Composition: $Al_{0.50}Ga_{0.50}As$
Side barrier layer 12
Thickness: 25 angstrom
Composition: $Al_{0.30}Ga_{0.70}As$
Quantum well layer 13
Thickness: 55 angstrom
Composition: GaAs
Barrier layer 14
Thickness: 50 angstrom
Composition: $Al_{0.30}Ga_{0.70}As$
n-type barrier layer 3
Thickness: 330 angstrom
Composition: $Al_{0.50}Ga_{0.50}As$

FIG. 25 illustrates a guided mode profile (near-field pattern) in the direction vertical to the epitaxy layer with respect to the structure shown in this embodiment. FIG. 26 shows a measured result in the radiation mode.

(Embodiment 10)

As illustrated in FIG. 11, the n-type buffer layer 10 having a thickness of 0.5 μm is formed on the n-type substrate 8 composed of GaAs. Formed sequentially on this layer are the n-type clad layer 1, the n-type light wave guide layer 2, the n-type barrier layer 3, the active layer 4, the p-type barrier layer 5, the p-type light wave guide layer 6 and the p-type clad layer 7. The n-type cap layer 11 is formed as an uppermost layer thereon.

The following are concrete configurations of the respective layers.

n-type cap layer 11
Thickness: 0.3 μm
Composition: GaAs

p-type clad layer 7
Thickness: 1.0 μm
Composition: $Al_{0.35}Ga_{0.65}As$
p-type light wave guide layer 6
Thickness: 0.46 μm
Composition: $Al_{0.30}Ga_{0.70}As$
n-type light wave guide layer 2
Thickness: 0.46 μm
Composition: $Al_{0.30}Ga_{0.70}As$
n-type clad layer 1
Thickness: 1.0 μm
Composition: $Al_{0.35}Ga_{0.65}As$
n-type buffer layer 10
Thickness: 0.5 μm
Composition: GaAs
n-type substrate 8
Composition: (100) GaAs

The active layer 4 is formed such that the 4-layered quantum well layers 13 are each partitioned by the barrier layers 14 between the side barrier layers 12 deposited on the inner walls of the respective barrier layers 5, 3 in the area sandwiched in between the p-type barrier layer 5 and the n-type barrier layer 3. The concrete configurations of this active layer 4 are given as follows: p-type barrier layer 5
Thickness: 500 angstrom
Composition: $Al_{0.50}Ga_{0.50}As$
Side barrier layer 12
Thickness: 25 angstrom
Composition: $Al_{0.30}Ga_{0.70}As$
Quantum well layer 13
Thickness: 55 angstrom
Composition: GaAs
Barrier layer 14
Thickness: 50 angstrom
Composition: $Al_{0.30}Ga_{0.70}As$
n-type barrier layer 3
Thickness: 500 angstrom
Composition: $Al_{0.50}Ga_{0.50}As$

FIG. 25 illustrates a guided mode profile (near-field pattern) in the direction vertical to the epitaxy layer with respect to the structure shown in this embodiment. FIG. 26 shows a measured result in the radiation mode.

(Embodiment 11)

As illustrated in FIG. 12, the n-type buffer layer 10 having a thickness of 0.5 μm is formed on the n-type substrate 8 composed of GaAs. Formed sequentially on this layer are the n-type clad layer 1, the n-type light wave guide layer 2, the n-type barrier layer 3, the active layer 4, the p-type barrier layer 5, the p-type light wave guide layer 6 and the p-type clad layer 7. The n-type cap layer 11 is formed as an uppermost layer thereon.

The following are concrete configurations of the respective layers.
n-type cap layer 11
Thickness: 0.3 μm
Composition: GaAs
p-type clad layer 7
Thickness: 1.0 μm
Composition: $Al_{0.35}Ga_{0.65}As$
p-type light wave guide layer 6
Thickness: 0.46 μm
Composition: $Al_{0.25}Ga_{0.75}As$
n-type light wave guide layer 2
Thickness: 0.46 μm

Composition: $Al_{0.25}Ga_{0.75}As$
n-type clad layer 1
Thickness: 1.0 μm
Composition: $Al_{0.35}Ga_{0.65}As$
n-type buffer layer 10
Thickness: 0.5 μm
Composition: GaAs
n-type substrate 8
Composition: (100) GaAs

The active layer 4 is formed such that the 4-layered quantum well layers 13 are each partitioned by the barrier layers 14 between the side barrier layers 12 deposited on the inner walls of the respective barrier layers 5, 3 in the area sandwiched in between the p-type barrier layer 5 and the n-type barrier layer 3. The concrete configurations of this active layer 4 are given as follows:

p-type barrier layer 5
Thickness: 50 angstrom
Composition: $Al_{0.50}Ga_{0.50}As$
Side barrier layer 12
Thickness: 25 angstrom
Composition: $Al_{0.25}Ga_{0.75}As$
Quantum well layer 13
Thickness: 55 angstrom
Composition: GaAs
Barrier layer 14
Thickness: 50 angstrom
Composition: $Al_{0.25}Ga_{0.75}As$
n-type barrier layer 3
Thickness: 50 angstrom
Composition: $Al_{0.50}Ga_{0.50}As$

FIG. 27 illustrates a guided mode profile (near-field pattern) in the direction vertical to the epitaxy layer with respect to the structure shown in this embodiment. FIG. 28 shows a measured result in the radiation mode.

(Embodiment 12)

As illustrated in FIG. 13, the n-type buffer layer 10 having a thickness of 0.5 μm is formed on the n-type substrate 8 composed of GaAs. Formed sequentially on this layer are the n-type clad layer 1, the n-type light wave guide layer 2, the n-type barrier layer 3, the active layer 4, the p-type barrier layer 5, the p-type light wave guide layer 6 and the p-type clad layer 7. The n-type cap layer 11 is formed as an uppermost layer thereon.

The following are concrete configurations of the respective layers.

n-type cap layer 11
Thickness: 0.3 μm
Composition: GaAs
p-type clad layer 7
Thickness: 1.0 μm
Composition: $Al_{0.35}Ga_{0.65}As$
p-type light wave guide layer 6
Thickness: 0.46 μm
Composition: $Al_{0.25}Ga_{0.75}As$
n-type light wave guide layer 2
Thickness: 0.46 μm
Composition: $Al_{0.25}Ga_{0.75}As$
n-type clad layer 1
Thickness: 1.0 μm
Composition: $Al_{0.35}Ga_{0.65}As$
n-type buffer layer 10
Thickness: 0.5 μm
Composition: GaAs

n-type substrate 8
Composition: (100) GaAs
The active layer 4 is formed such that the 4-layered quantum well layers 13 are each partitioned by the barrier layers 14 between the side barrier layers 12 deposited on the inner walls of the respective barrier layers 5, 3 in the area sandwiched in between the p-type barrier layer 5 and the n-type barrier layer 3. The concrete configurations of this active layer 4 are given as follows:
p-type barrier layer 5
Thickness: 135 angstrom
Composition: $Al_{0.50}Ga_{0.50}As$
Side barrier layer 12
Thickness: 25 angstrom
Composition: $Al_{0.25}Ga_{0.75}As$
Quantum well layer 13
Thickness: 55 angstrom
Composition: GaAs
Barrier layer 14
Thickness: 50 angstrom
Composition: $Al_{0.25}Ga_{0.75}As$
n-type barrier layer 3
Thickness: 135 angstrom
Composition: $Al_{0.50}Ga_{0.50}As$
FIG. 27 illustrates a guided mode profile (near-field pattern) in the direction vertical to the epitaxy layer with respect to the structure shown in this embodiment. FIG. 28 shows a measured result in the radiation mode.

(Embodiment 13)

As illustrated in FIG. 14, the n-type buffer layer 10 having a thickness of 0.5 μm is formed on the n-type substrate 8 composed of GaAs. Formed sequentially on this layer are the n-type clad layer 1, the n-type light wave guide layer 2, the n-type barrier layer 3, the active layer 4, the p-type barrier layer 5, the p-type light wave guide layer 6 and the p-type clad layer 7. The n-type cap layer 11 is formed as an uppermost layer thereon.
The following are concrete configurations of the respective layers.
n-type cap layer 11
Thickness: 0.3 μm
Composition: GaAs
p-type clad layer 7
Thickness: 1.0 μm
Composition: $Al_{0.35}Ga_{0.65}As$
p-type light wave guide layer 6
Thickness: 0.46 μm
Composition: $Al_{0.25}Ga_{0.75}As$
n-type light wave guide layer 2
Thickness: 0.46 μm
Composition: $Al_{0.25}Ga_{0.75}As$
n-type clad layer 1
Thickness: 1.0 μm
Composition: $Al_{0.35}Ga_{0.65}As$
n-type buffer layer 10
Thickness: 0.5 μm
Composition: GaAs
n-type substrate 8
Composition: (100) GaAs
The active layer 4 is formed such that the 4-layered quantum well layers 13 are each partitioned by the barrier layers 14 between the side barrier layers 12 deposited on the inner walls of the respective barrier layers 5, 3 in the area sandwiched in between the p-type barrier layer 5 and the n-type barrier layer 3. The concrete configurations of this active layer 4 are given as follows:
p-type barrier layer 5

Thickness: 200 angstrom
Composition: $Al_{0.50}Ga_{0.50}As$
Side barrier layer 12
Thickness: 25 angstrom
Composition: $Al_{0.25}Ga_{0.75}As$
Quantum well layer 13
Thickness: 55 angstrom
Composition: GaAs
Barrier layer 14
Thickness: 50 angstrom
Composition: $Al_{0.25}Ga_{0.75}As$
n-type barrier layer 3
Thickness: 200 angstrom
Composition: $Al_{0.50}Ga_{0.50}As$

FIG. 27 illustrates a guided mode profile (near-field pattern) in the direction vertical to the epitaxy layer with respect to the structure shown in this embodiment. FIG. 28 shows a measured result in the radiation mode.

(Embodiment 14)

As illustrated in FIG. 15, the n-type buffer layer 10 having a thickness of 0.5 μm is formed on the n-type substrate 8 composed of GaAs. Formed sequentially on this layer are the n-type clad layer 1, the n-type light wave guide layer 2, the n-type barrier layer 3, the active layer 4, the p-type barrier layer 5, the p-type light wave guide layer 6 and the p-type clad layer 7. The n-type cap layer 11 is formed as an uppermost layer thereon.

The following are concrete configurations of the respective layers.

n-type cap layer 11
Thickness: 0.3 μm
Composition: GaAs
p-type clad layer 7
Thickness: 1.0 μm
Composition: $Al_{0.35}Ga_{0.65}As$
p-type light wave guide layer 6
Thickness: 0.46 μm
Composition: $Al_{0.25}Ga_{0.75}As$
n-type light wave guide layer 2
Thickness: 0.46 μm
Composition: $Al_{0.25}Ga_{0.75}As$
n-type clad layer 1
Thickness: 1.0 μm
Composition: $Al_{0.35}Ga_{0.65}As$
n-type buffer layer 10
Thickness: 0.5 μm
Composition: GaAs
n-type substrate 8
Composition: (100) GaAs

The active layer 4 is formed such that the 4-layered quantum well layers 13 are each partitioned by the barrier layers 14 between the side barrier layers 12 deposited on the inner walls of the respective barrier layers 5, 3 in the area sandwiched in between the p-type barrier layer 5 and the n-type barrier layer 3. The concrete configurations of this active layer 4 are given as follows:

p-type barrier layer 5
Thickness: 330 angstrom
Composition: $Al_{0.50}Ga_{0.50}As$
Side barrier layer 12
Thickness: 25 angstrom
Composition: $Al_{0.25}Ga_{0.75}As$
Quantum well layer 13
Thickness: 55 angstrom

Composition: GaAs
Barrier layer 14
Thickness: 50 angstrom
Composition: $Al_{0.25}Ga_{0.75}As$
n-type barrier layer 3
Thickness: 330 angstrom
Composition: $Al_{0.50}Ga_{0.50}As$

FIG. 27 illustrates a guided mode profile (near-field pattern) in the direction vertical to the epitaxy layer with respect to the structure shown in this embodiment. FIG. 28 shows a measured result in the radiation mode.

(Embodiment 15)

As illustrated in FIG. 16, the n-type buffer layer 10 having a thickness of 0.5 μm is formed on the n-type substrate 8 composed of GaAs. Formed sequentially on this layer are the n-type clad layer 1, the n-type light wave guide layer 2, the n-type barrier layer 3, the active layer 4, the p-type barrier layer 5, the p-type light wave guide layer 6 and the p-type clad layer 7. The n-type cap layer 11 is formed as an uppermost layer thereon.

The following are concrete configurations of the respective layers.

n-type cap layer 11
Thickness: 0.3 μm
Composition: GaAs
p-type clad layer 7
Thickness: 1.0 μm
Composition: $Al_{0.35}Ga_{0.65}As$
p-type light wave guide layer 6
Thickness: 0.46 μm
Composition: $Al_{0.25}Ga_{0.75}As$
n-type light wave guide layer 2
Thickness: 0.46 μm
Composition: $Al_{0.25}Ga_{0.75}As$
n-type clad layer 1
Thickness: 1.0 μm
Composition: $Al_{0.35}Ga_{0.65}As$
n-type buffer layer 10
Thickness: 0.5 μm
Composition: GaAs
n-type substrate 8
Composition: (100) GaAs

The active layer 4 is formed such that the 4-layered quantum well layers 13 are each partitioned by the barrier layers 14 between the side barrier layers 12 deposited on the inner walls of the respective barrier layers 5, 3 in the area sandwiched in between the p-type barrier layer 5 and the n-type barrier layer 3. The concrete configurations of this active layer 4 are given as follows:

p-type barrier layer 5
Thickness: 50 angstrom
Composition: $Al_{0.65}Ga_{0.35}As$
Side barrier layer 12
Thickness: 25 angstrom
Composition: $Al_{0.25}Ga_{0.75}As$
Quantum well layer 13
Thickness: 55 angstrom
Composition: GaAs
Barrier layer 14
Thickness: 50 angstrom
Composition: $Al_{0.25}Ga_{0.75}As$
n-type barrier layer 3
Thickness: 50 angstrom
Composition: $Al_{0.65}Ga_{0.35}As$

FIG. 29 illustrates a guided mode profile (near-field pattern) in the direction vertical to the epitaxy layer with respect to the structure shown in this embodiment. FIG. 30 shows a measured result in the radiation mode.

(Embodiment 16)

As illustrated in FIG. 17, the n-type buffer layer 10 having a thickness of 0.5 μm is formed on the n-type substrate 8 composed of GaAs. Formed sequentially on this layer are the n-type clad layer 1, the n-type light wave guide layer 2, the n-type barrier layer 3, the active layer 4, the p-type barrier layer 5, the p-type light wave guide layer 6 and the p-type clad layer 7. The n-type cap layer 11 is formed as an uppermost layer thereon.

The following are concrete configurations of the respective layers.

n-type cap layer 11
- Thickness: 0.3 μm
- Composition: GaAs

p-type clad layer 7
- Thickness: 1.0 μm
- Composition: $Al_{0.35}Ga_{0.65}As$

p-type light wave guide layer 6
- Thickness: 0.46 μm
- Composition: $Al_{0.25}Ga_{0.75}As$

n-type light wave guide layer 2
- Thickness: 0.46 μm
- Composition: $Al_{0.25}Ga_{0.75}As$

n-type clad layer 1
- Thickness: 1.0 μm
- Composition: $Al_{0.35}Ga_{0.65}As$

n-type buffer layer 10
- Thickness: 0.5 μm
- Composition: GaAs

n-type substrate 8
- Composition: (100) GaAs

The active layer 4 is formed such that the 4-layered quantum well layers 13 are each partitioned by the barrier layers 14 between the side barrier layers 12 deposited on the inner walls of the respective barrier layers 5, 3 in the area sandwiched in between the p-type barrier layer 5 and the n-type barrier layer 3. The concrete configurations of this active layer 4 are given as follows:

p-type barrier layer 5
- Thickness: 100 angstrom
- Composition: $Al_{0.35}Ga_{0.65}As$

Side barrier layer 12
- Thickness: 25 angstrom
- Composition: $Al_{0.25}Ga_{0.75}As$

Quantum well layer 13
- Thickness: 55 angstrom
- Composition: GaAs

Barrier layer 14
- Thickness: 50 angstrom
- Composition: $Al_{0.25}Ga_{0.75}As$

n-type barrier layer 3
- Thickness: 100 angstrom
- Composition: $Al_{0.35}Ga_{0.65}As$

FIG. 29 illustrates a guided mode profile (near-field pattern) in the direction vertical to the epitaxy layer with respect to the structure shown in this embodiment. FIG. 30 shows a measured result in the radiation mode.

(Embodiment 17)

As illustrated in FIG. 18, the n-type buffer layer 10 having a thickness of 0.5 μm is formed on the n-type substrate 8 composed of GaAs. Formed sequentially on this layer are the n-type clad layer 1, the n-type light wave guide layer 2, the n-type barrier layer 3, the active layer 4, the p-type barrier layer 5, the p-type light wave guide layer 6 and the p-type clad layer 7. The n-type cap layer 11 is formed as an uppermost layer thereon.

The following are concrete configurations of the respective layers.

n-type cap layer 11
Thickness: 0.3 μm
Composition: GaAs
p-type clad layer 7
Thickness: 1.0 μm
Composition: $Al_{0.35}Ga_{0.65}As$
p-type light wave guide layer 6
Thickness: 0.46 μm
Composition: $Al_{0.25}Ga_{0.75}As$
n-type light wave guide layer 2
Thickness: 0.46 μm
Composition: $Al_{0.25}Ga_{0.75}As$
n-type clad layer 1
Thickness: 1.0 μm
Composition: $Al_{0.35}Ga_{0.65}As$
n-type buffer layer 10
Thickness: 0.5 μm
Composition: GaAs
n-type substrate 8
Composition: (100) GaAs

The active layer 4 is formed such that the 4-layered quantum well layers 13 are each partitioned by the barrier layers 14 between the side barrier layers 12 deposited on the inner walls of the respective barrier layers 5, 3 in the area sandwiched in between the p-type barrier layer 5 and the n-type barrier layer 3. The concrete configurations of this active layer 4 are given as follows:

p-type barrier layer 5
Thickness: 200 angstrom
Composition: $Al_{0.65}Ga_{0.35}As$
Side barrier layer 12
Thickness: 25 angstrom
Composition: $Al_{0.25}Ga_{0.75}As$
Quantum well layer 13
Thickness: 55 angstrom
Composition: GaAs
Barrier layer 14
Thickness: 50 angstrom
Composition: $Al_{0.25}Ga_{0.75}As$
n-type barrier layer 3
Thickness: 200 angstrom
Composition: $Al_{0.65}Ga_{0.35}As$

FIG. 29 illustrates a guided mode profile (near-field pattern) in the direction vertical to the epitaxy layer with respect to the structure shown in this embodiment. FIG. 30 shows a measured result in the radiation mode.

(Embodiment 18)

As illustrated in FIG. 19, the n-type buffer layer 10 having a thickness of 0.5 μm is formed on the n-type substrate 8 composed of GaAs. Formed sequentially on this layer are the n-type clad layer 1, the n-type light wave guide layer 2, the n-type barrier layer 3, the active layer 4, the p-type barrier layer 5, the p-type light wave guide layer 6 and the p-type clad layer 7. The n-type cap layer 11 is formed as an uppermost layer thereon.

The following are concrete configurations of the respective layers.

n-type cap layer 11
Thickness: 0.3 μm
Composition: GaAs

p-type clad layer 7
Thickness: 1.0 μm
Composition: $Al_{0.35}Ga_{0.65}As$

p-type light wave guide layer 6
Thickness: 0.46 μm
Composition: $Al_{0.25}Ga_{0.75}As$

n-type light wave guide layer 2
Thickness: 0.46 μm
Composition: $Al_{0.25}Ga_{0.75}As$

n-type clad layer 1
Thickness: 1.0 μm
Composition: $Al_{0.35}Ga_{0.65}As$

n-type buffer layer 10
Thickness: 0.5 μm
Composition: GaAs

n-type substrate 8
Composition: (100) GaAs

The active layer 4 is formed such that the 4-layered quantum well layers 13 are each partitioned by the barrier layers 14 between the side barrier layers 12 deposited on the inner walls of the respective barrier layers 5, 3 in the area sandwiched in between the p-type barrier layer 5 and the n-type barrier layer 3. The concrete configurations of this active layer 4 are given as follows:

p-type barrier layer 5
Thickness: 280 angstrom
Composition: $Al_{0.65}Ga_{0.35}As$

Side barrier layer 12
Thickness: 25 angstrom
Composition: $Al_{0.25}Ga_{0.75}As$

Quantum well layer 13
Thickness: 55 angstrom
Composition: GaAs

Barrier layer 14
Thickness: 50 angstrom
Composition: $Al_{0.25}Ga_{0.75}As$

n-type barrier layer 3
Thickness: 280 angstrom
Composition: $Al_{0.65}Ga_{0.35}As$

FIG. 29 illustrates a guided mode profile (near-field pattern) in the direction vertical to the epitaxy layer with respect to the structure shown in this embodiment. FIG. 30 shows a measured result in the radiation mode.

(Comparative Example)

FIG. 20 is a schematic plan view showing a composition of a quantum well type laser element based on a conventional structure which is manufactured for comparisons with the above-mentioned embodiments 1 ~ 18.

The following are concrete configurations of the respective layers.

n-type cap layer 11
Thickness: 0.3 μm
Composition: GaAs

p-type clad layer 7
Thickness: 1.5 μm
Composition: $Al_{0.65}Ga_{0.35}As$

n-type clad layer 1
Thickness: 1.5 μm

Composition: $Al_{0.65}Ga_{0.35}As$

n-type buffer layer 10

Thickness: 0.5 μm

Composition: GaAs

n-type substrate 8

Composition: (100) GaAs

An active layer 4 is formed such that 4-layered quantum well layers 13 are partitioned by barrier layers 14 in an area sandwiched in between side barrier layers 12. The concrete configurations of this active layer 4 are given as follows:

Side barrier layer 12

Thickness: 120 angstrom

Composition: $Al_{0.30}Ga_{0.70}As$

Quantum well layer 13

Thickness: 50 angstrom

Composition: GaAs

Barrier layer 14

Thickness: 50 angstrom

Composition: $Al_{0.30}Ga_{0.70}As$

FIG. 21 illustrates a guided mode profile (near-field pattern) in the direction vertical to the epitaxy layer with respect to the structure shown in this embodiment. FIG. 22 shows a measured result in the radiation mode.

As obvious from FIG. 21, the weakly guiding semiconductor laser exhibits a center-pointed characteristic curve having exponential function tails on both sides. In contrast, the embodiments 1 ~ 18 exhibit characteristic forms similar to a hanging-bell-like Gaussian beam. For this reason, in the case of using the semiconductor laser in the present embodiment, there increases the beam intensity in the active layer 4 (mode center) where an optical damage is caused even with a mode expansion to the same extent as that in the prior arts. As shown by the measured results in Table 1 which follows, a level of the optical damage can be remarkably raised. Namely, a reduction in radiation angle and a remarkable improvement in the level of the optical damage in the present embodiments 1 ~ 3 become more apparent than in the comparative example. Note that an oscillation wavelength (angstrom) of the laser is approximately 800 nm in Table 1. Further, the optical damage level and the slope efficiency are each optical outputs per edge surface.

TABLE 1

| LD TYPE | NORMALIZED FREQUENCY | RADIATION ANGLE $\theta \perp$ / $\theta \parallel$ | OPTICAL DAMAGE (mW) | THRESHOLD CURRENT (mA) | SLOPE EFFICIENCY (mW/mA) |
|---|---|---|---|---|---|
| EMBODIMENT 1 | 1.6 | 25° | 250mW | 90mA | 0.5 |
| STRUCTURE IN FIG. 2 | | 5° | | | |
| EMBODIMENT 2 | 1.6 | 14° | 500mW | 300mA | 0.5 |
| STRUCTURE IN FIG. 3 | | 4° | | | |
| EMBODIMENT 3 | 3.5 | 18° | 400mW | 250mA | 0.5 |
| STRUCTURE IN FIG. 4 | | 5° | | | |
| COMPARATIVE EXAMPLE | 0.28 | 22° | 100mW | 75mA | 0.4 |
| STRUCTURE IN FIG. 20 | | 8° | | | |

## Industrial Applicability

In the industrial fields where the high-output semiconductor laser is employed for communications, optical recording on optical disks or the like, laser printers, laser medical treatments and laser machining, etc. according to the present invention, the high-efficiency semiconductor laser exhibiting a good beam profile at the low radiation beam angle can be obtained. Besides, it is possible to manufacture the high-output semiconductor laser by avoiding the concurrent optical damage of the edge surface with a simple structure. Especially in the $Al_xGa_{1-x}As$ semiconductor laser, the Al composition of the wave guide layer can be reduced, thereby facilitating the manufacturing process.

For this reason, the element of the present invention can be utilized in the form of the high-efficiency semiconductor laser device. Furthermore, a semiconductor laser excitation solid-state laser device can be constructed as an excitation source of a solid-state laser. The solid-state laser may involve the use of laser mediums such as Nd:YAG and Nd:YLF. If the semiconductor laser is employed as an excitation source of the solid-state laser, the problem is a method of connecting the semiconductor laser to the laser medium. Generally, excitation beams from the semiconductor laser are focused at a high efficiency through such a lens as to mode-match an excitation volume of the semiconductor laser with a mode volume of the laser oscillator.

In the laser element according to this invention, the beams may be focused by use of the lens as described above. As illustrated in FIGS. 32 and 33, the excitation beams from a semiconductor laser element 21 can be made to strike on a laser medium 23 without effecting any optical processing on the excitation beams from the semiconductor laser element 21. Incidentally, the numeral 23 designates an output mirror. Note that FIG. 32 shows a direct-connection type wherein the semiconductor laser element 21 is connected directly to the laser medium 23, while FIG. 33 illustrates a fiber connection type semiconductor laser excitation solid-state laser device in which the semiconductor laser element 21 is connected via an optical fiber 22 to the laser medium 23.

## Claims

1. A semiconductor laser element in which an active layer incorporating a light guiding function, comprising:

   barrier layers, formed bilaterally externally of said active layer in section which is formed in the vertical direction from the surface of said element, for reducing the light guiding function of said active layer;

   wave guide layers provided bilaterally externally of said barrier layers and having bandgaps; and

   clad layers provided so that said wave guide layers are sandwiched in between said clad layers.

2. The semiconductor laser element according to claim 1, wherein said bandgap of said wave guide layer is a planar or spherical oblique bandgap which becomes narrower with a closer proximity to said barrier layer from the horizontal exterior in section.

3. The semiconductor laser element according to claim 1 or 2, wherein $V_1$, $V_2$ relative to the normalized frequency V in a guided mode are defined such as:

$$V_1 = \pi \cdot d_1 / \lambda \cdot (N_0^2 - N_2^2)^{0.5}$$
$$V_2 = \pi \cdot d_2 / \lambda \cdot (N_0^2 - N_3^2)^{0.5}$$

   where $\pi$ is the ratio of the circumference of a circle to its diameter, $d_1$ is the thickness of said barrier layer, $d_2$ is the thickness of said two clad layers, $\lambda$ is the oscillation wavelength, $N_0$ is the refractive index of said wave guide layer (however, if the refractive index of said wave guide layer continuously changes, the maximum value of $N_0$ is used), $N_1$ is the refractive index of said active layer, $N_2$ is the refractive index of said barrier layer, and $N_3$ is the refractive index of said clad layer, and then a relationship of $V_1 < V_2 / 10$ is established.

4. The semiconductor laser element according to claim 3, wherein an energy gap difference E (eV) between said wave guide layer and said barrier layer is given by:

$$E > (2.5 \times 10^3 / d_2)$$

   where d (angstrom) is the thickness of said barrier layer.

5. The semiconductor laser element according to claim 4, wherein $Al_xGa_{1-x}As$ ($0 \leq x < 1$) is employed, and the composition of said wave guide layer is:

   $Al_xGa_{1-x}As$ ($0 \leq x < 0.35$)

6. The semiconductor laser element according to claim 5, wherein when the composition of said wave guide layer is $Al_xGa_{1-x}As$ (however, $0 \leq x < 1$), a relationship between x and the thickness d (angstrom) of said barrier layer falls within the following ranges:

$$x > (2.2 \times 10^3 / d^2)$$

and

$$x < (5.0 \times 10^4 / d^2)$$

7. The semiconductor layer element according to claim 4, wherein $V_0$ is given by:

$$V_0 = \pi \cdot d_0 / \lambda \cdot (N_1^2 - N_0^2)^{0.5}$$

where $d_0$ is the thickness of said active layer, $V_0$ is, however, if said active layer is a quantum well, defined such as:

$$V_0 = N \cdot \pi \cdot d_0 / \lambda \, (N_1^2 - N_0^2)^{0.5}$$

where $d_0$ is the thickness of said quantum well layer, $N_1$ is the refractive index of said quantum well layer, $N_0$ is the refractive index of said wave guide layer, and N is the number of said quantum wells, and then a relationship of $(V_0 / 3) < V_1 < V_0$ is established.

8. A laser device using said semiconductor laser element according to any of claims 1 through 7.

9. A semiconductor laser excitation solid-state laser device using said semiconductor laser element according to any of claims 1 through 7 as a laser excitation light source.

10. The semiconductor laser excitation solid-state laser device according to claim 9, wherein the excitation light outputted from said laser element enters a solid-state laser without employing a lens.

FIG.1(a)

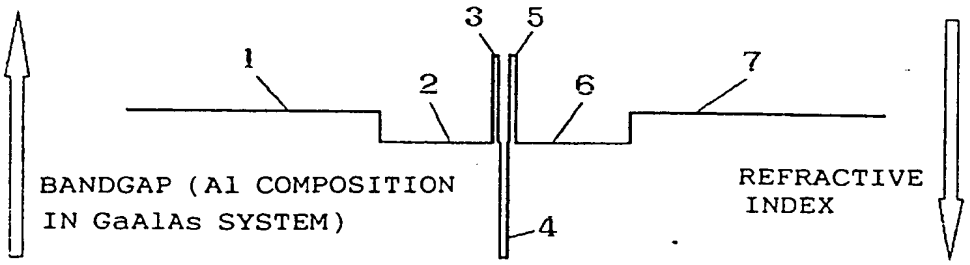


FIG.1(b)

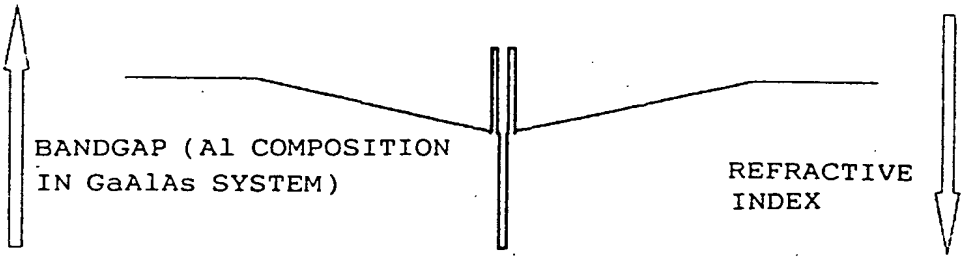


FIG.1(c)

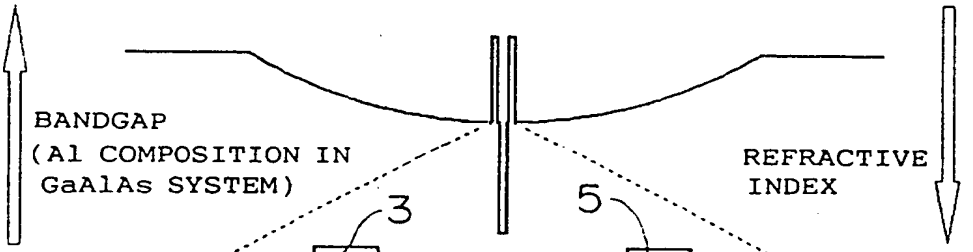


FIG.1(d)

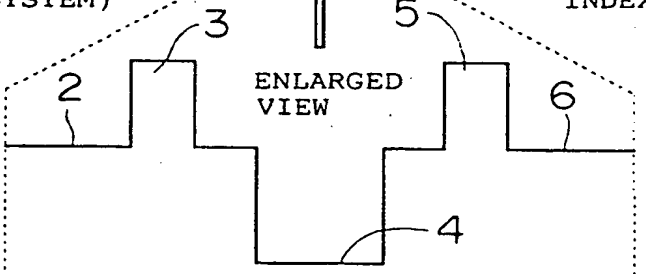


FIG.1(e)

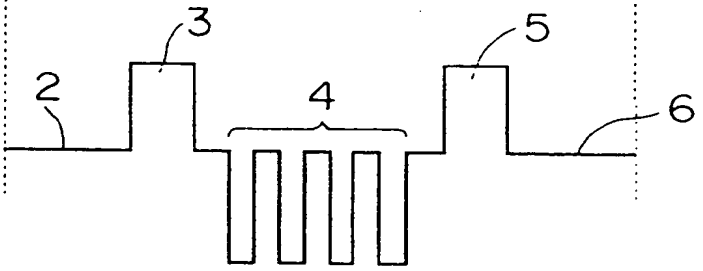

FIG.2

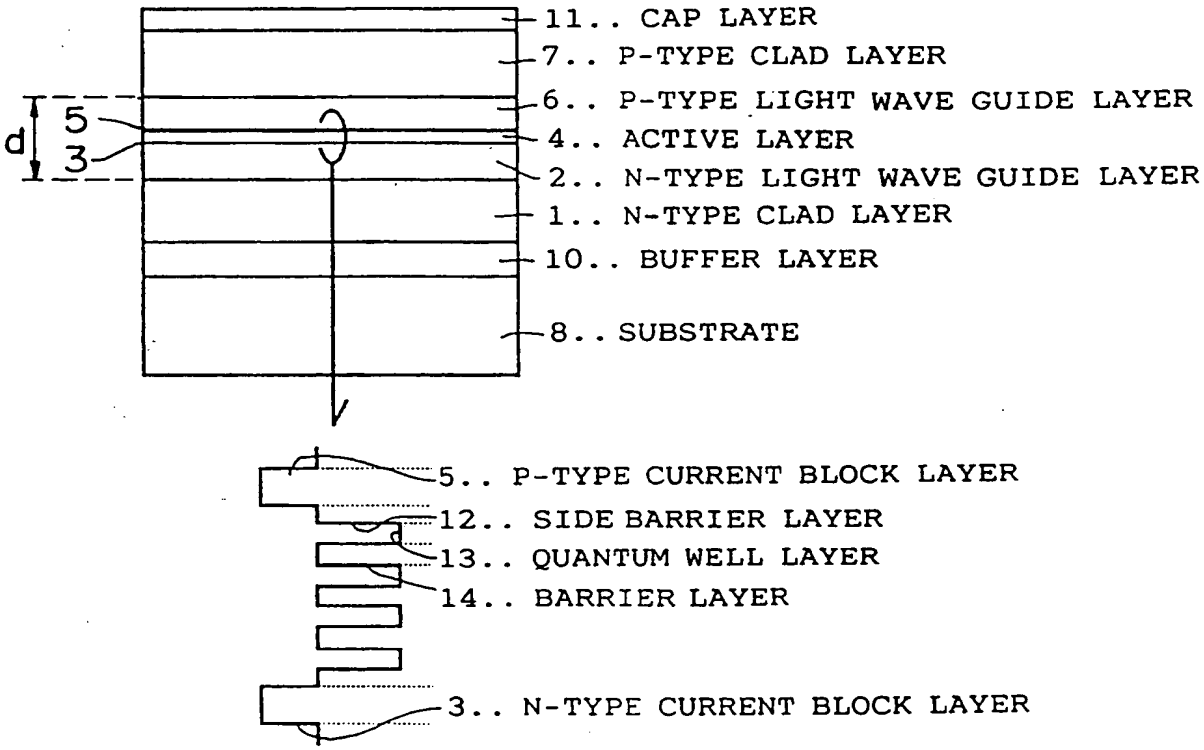


VIEW OF ACTIVE LAYER ENERGY BAND

FIG.3

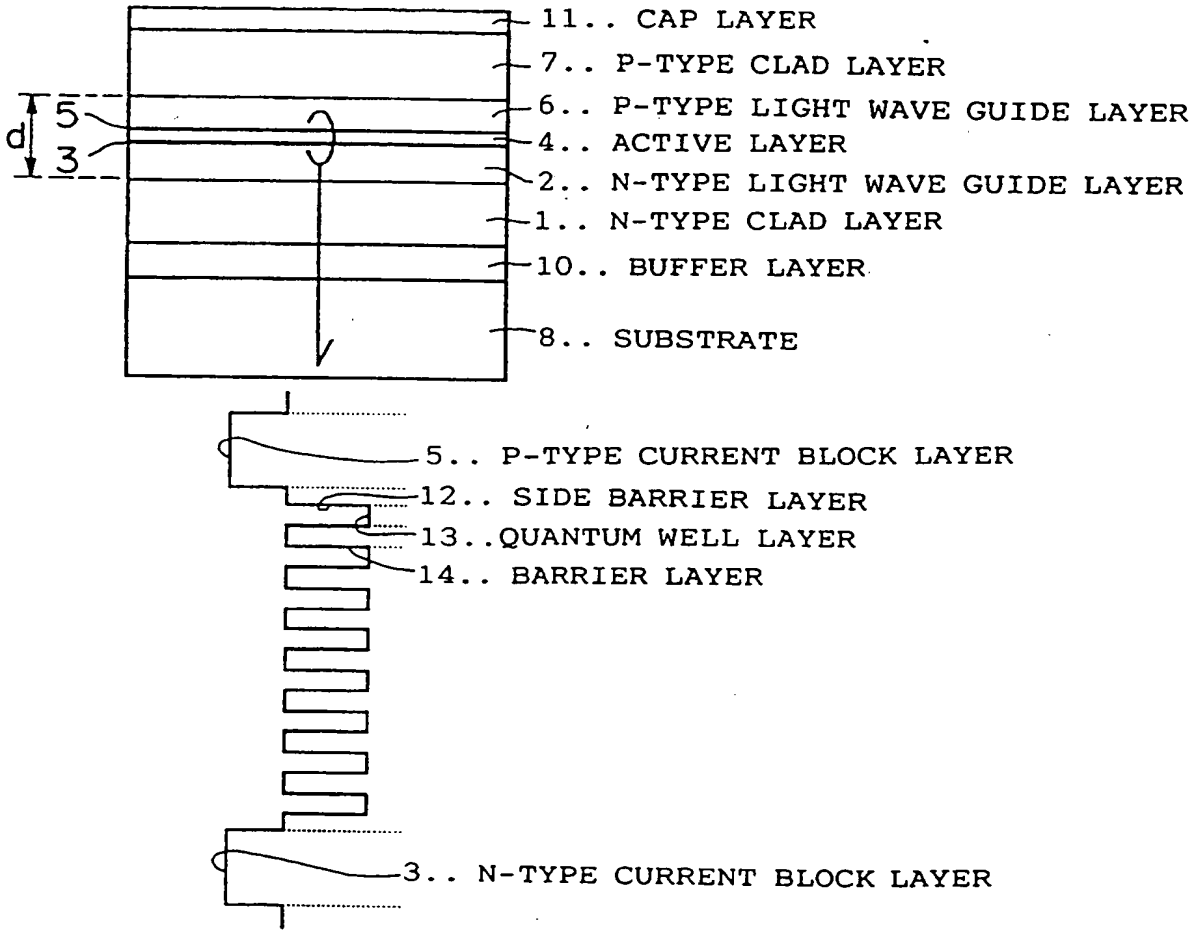


VIEW OF ACTIVE LAYER ENERGY BAND

FIG. 4

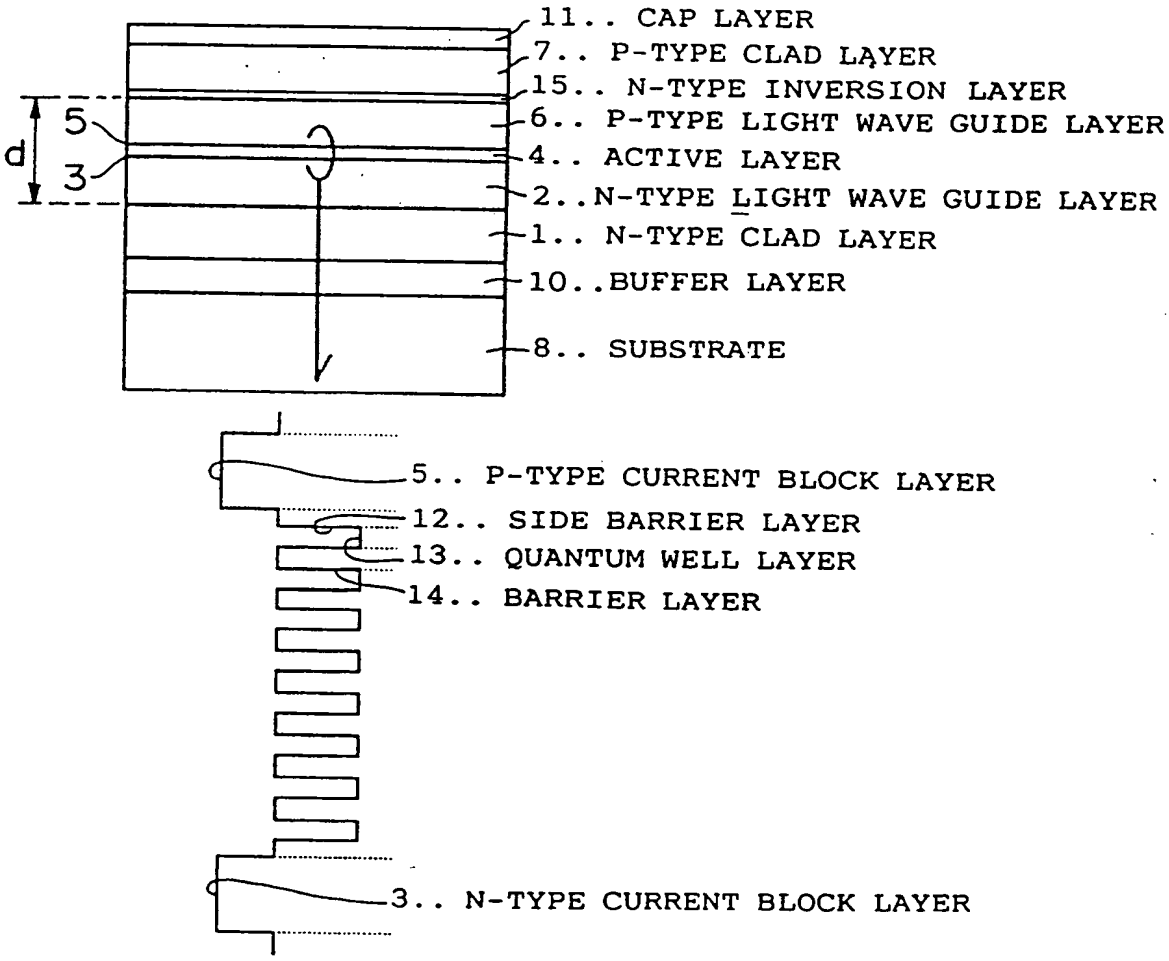


VIEW OF ACTIVE LAYER ENERGY BAND

FIG. 5

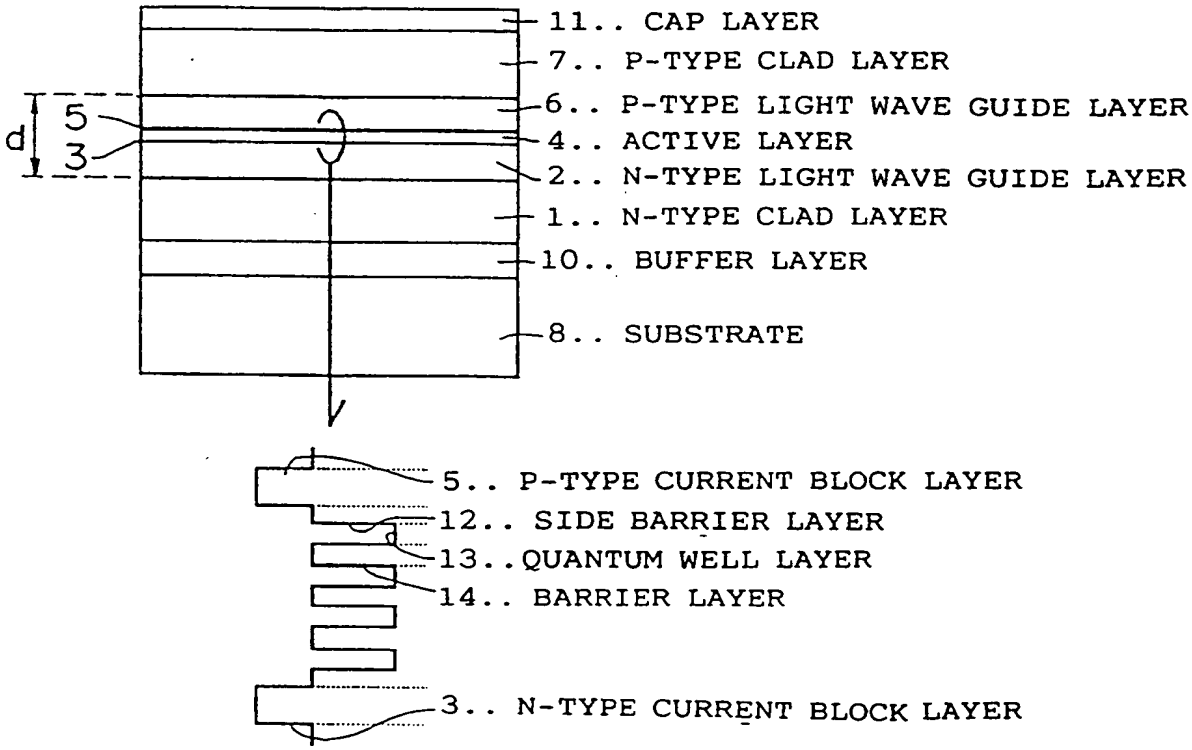


VIEW OF ACTIVE LAYER ENERGY BAND

FIG.6

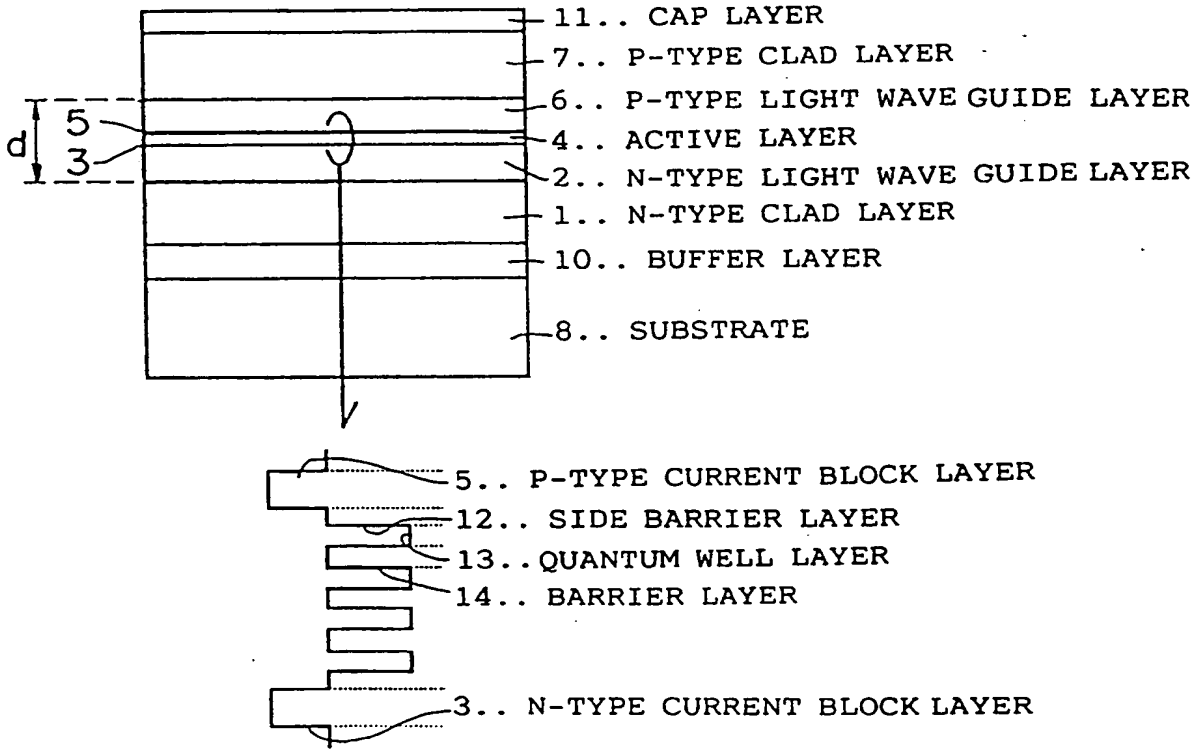


VIEW OF ACTIVE LAYER ENERGY BAND

FIG.7

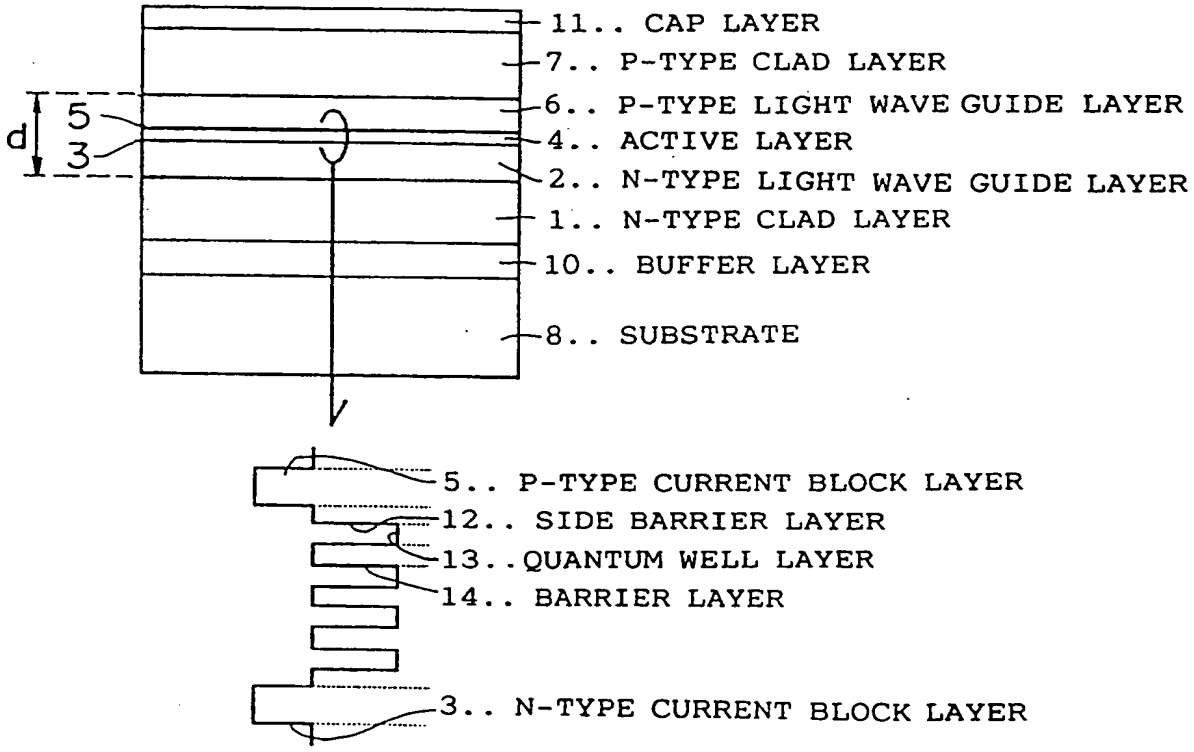


VIEW OF ACTIVE LAYER ENERGY BAND

FIG.8

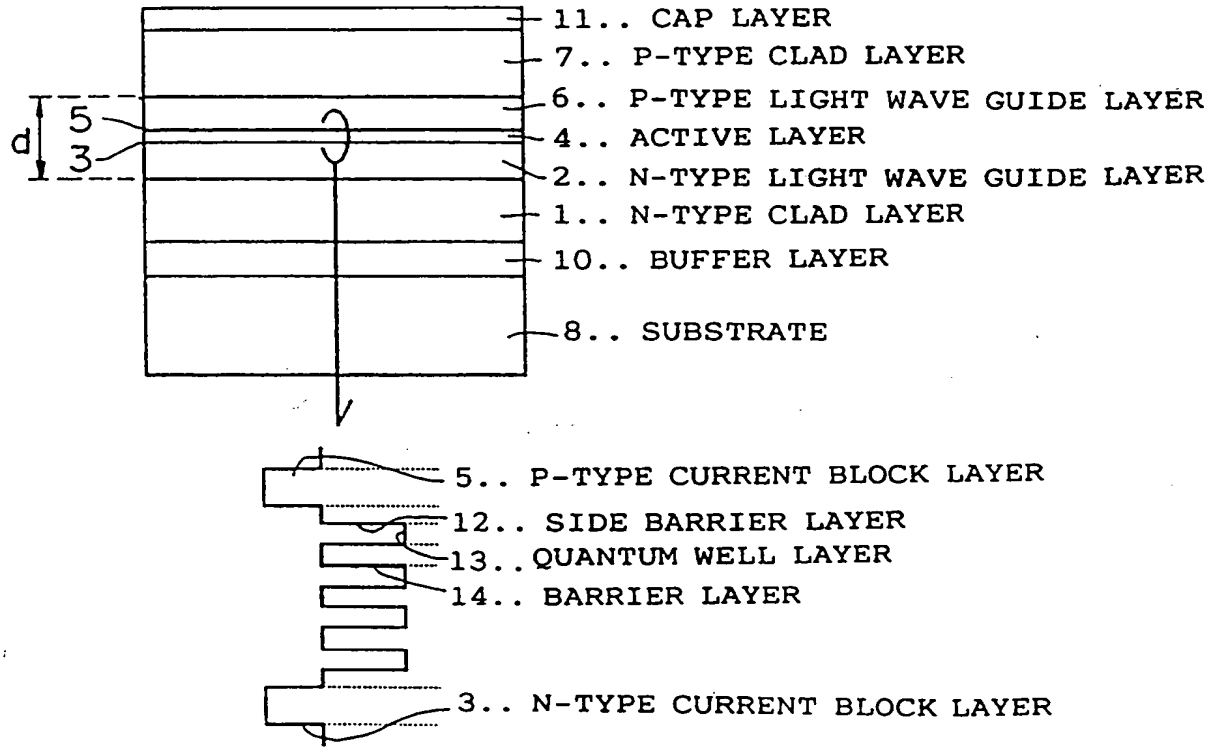


VIEW OF ACTIVE LAYER ENERGY BAND

FIG.9

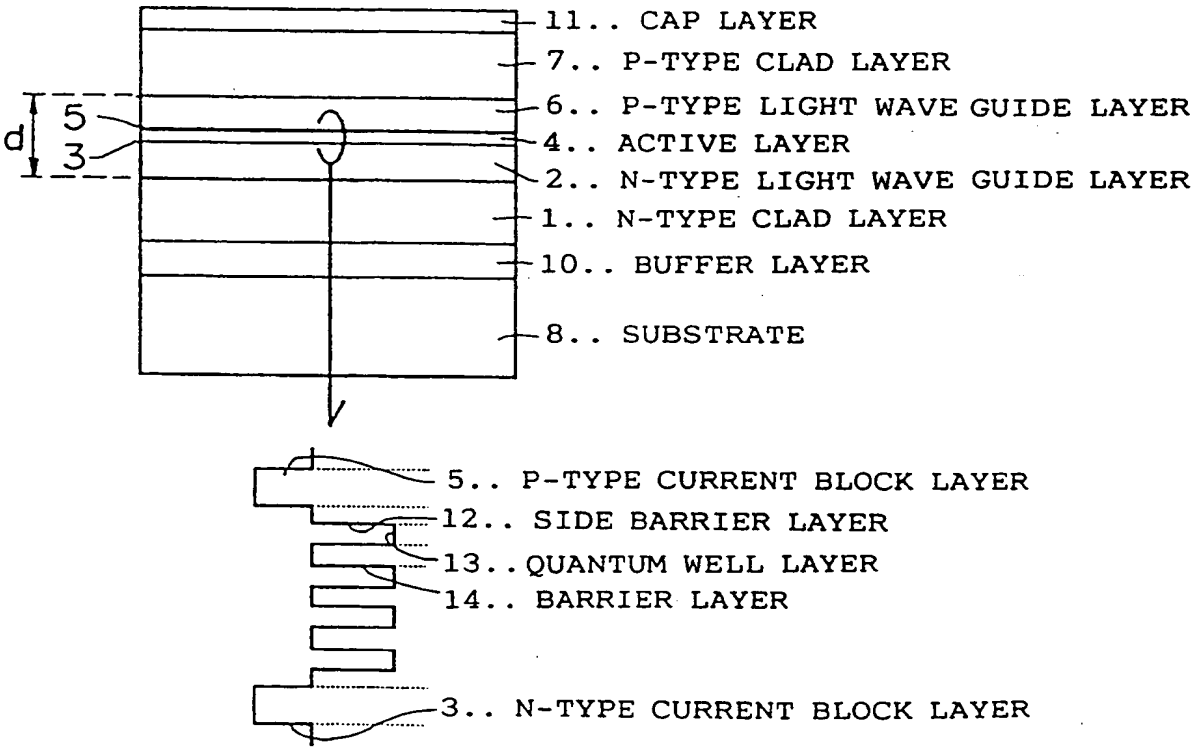


VIEW OF ACTIVE LAYER ENERGY BAND

FIG.10

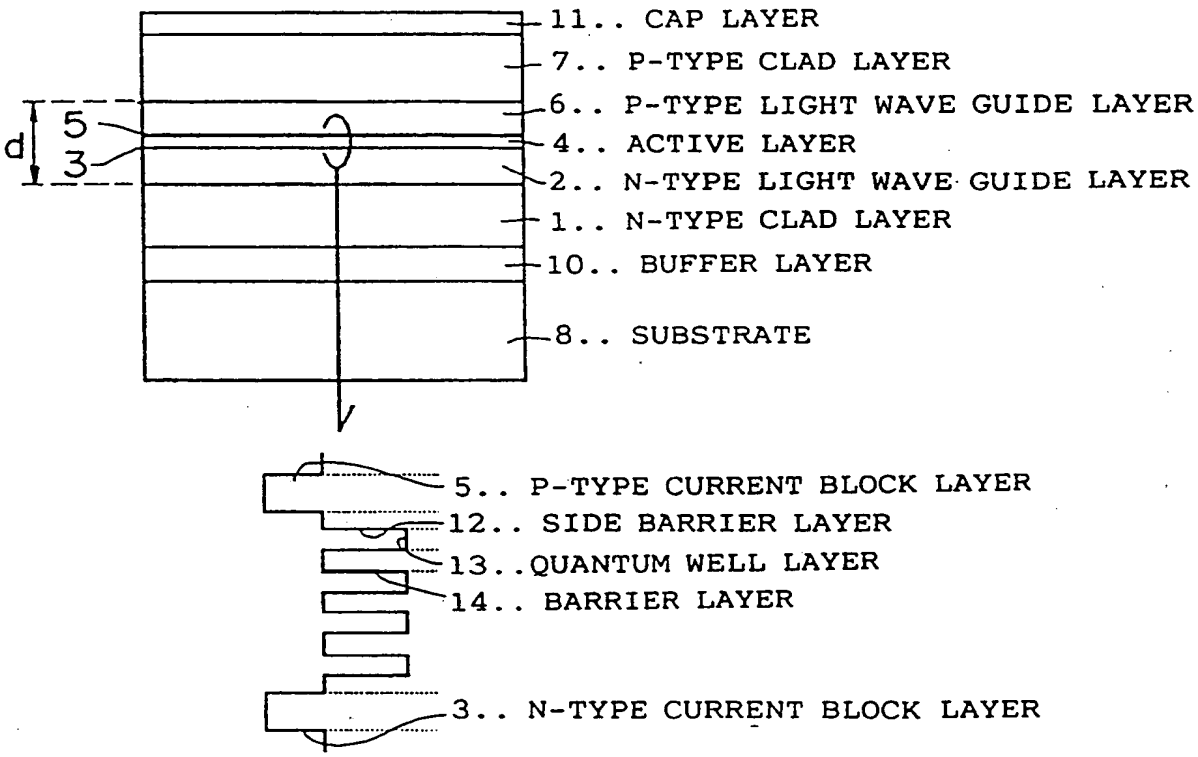


VIEW OF ACTIVE LAYER ENERGY BAND

FIG.11

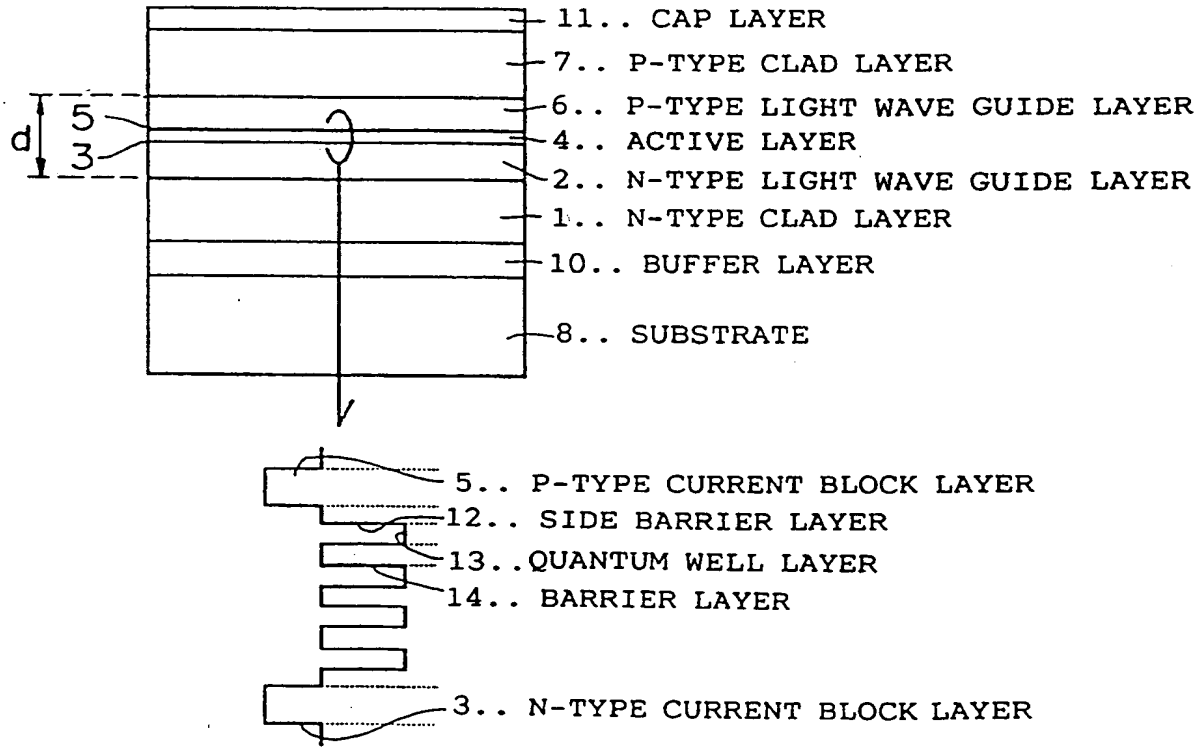


VIEW OF ACTIVE LAYER ENERGY BAND

FIG.12

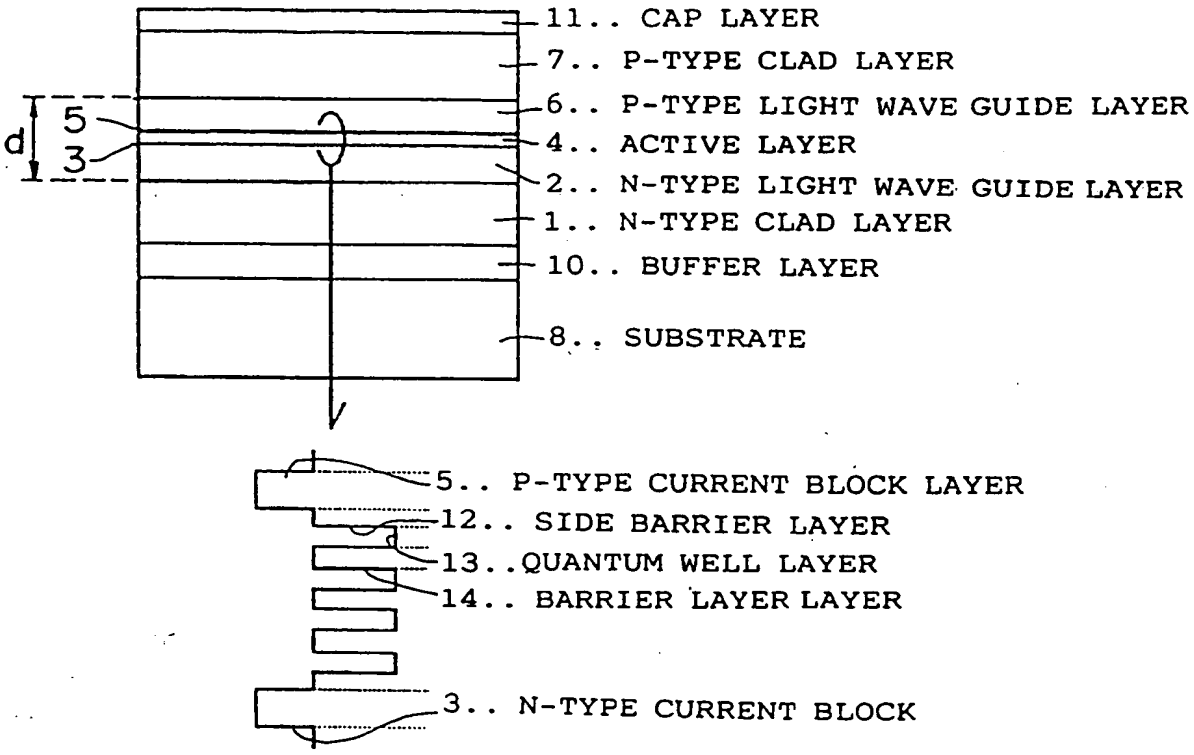


VIEW OF ACTIVE LAYER ENERGY BAND

FIG.13

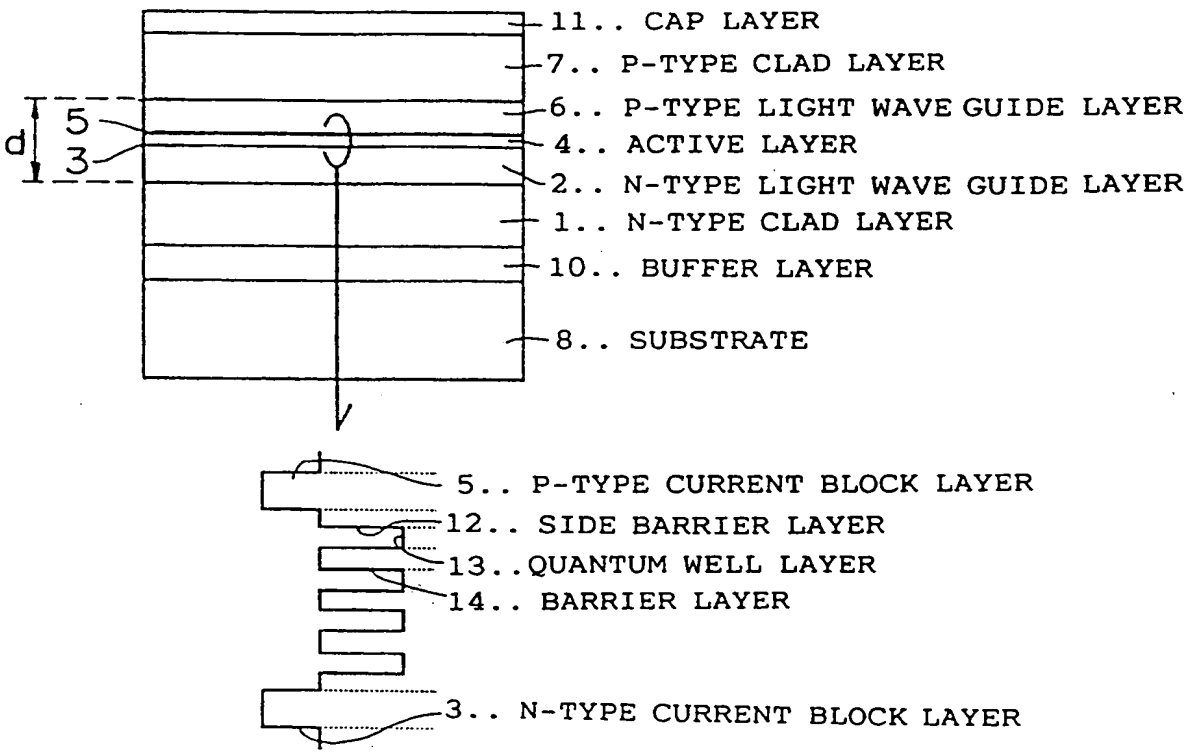


VIEW OF ACTIVE LAYER ENERGY BAND

FIG.14

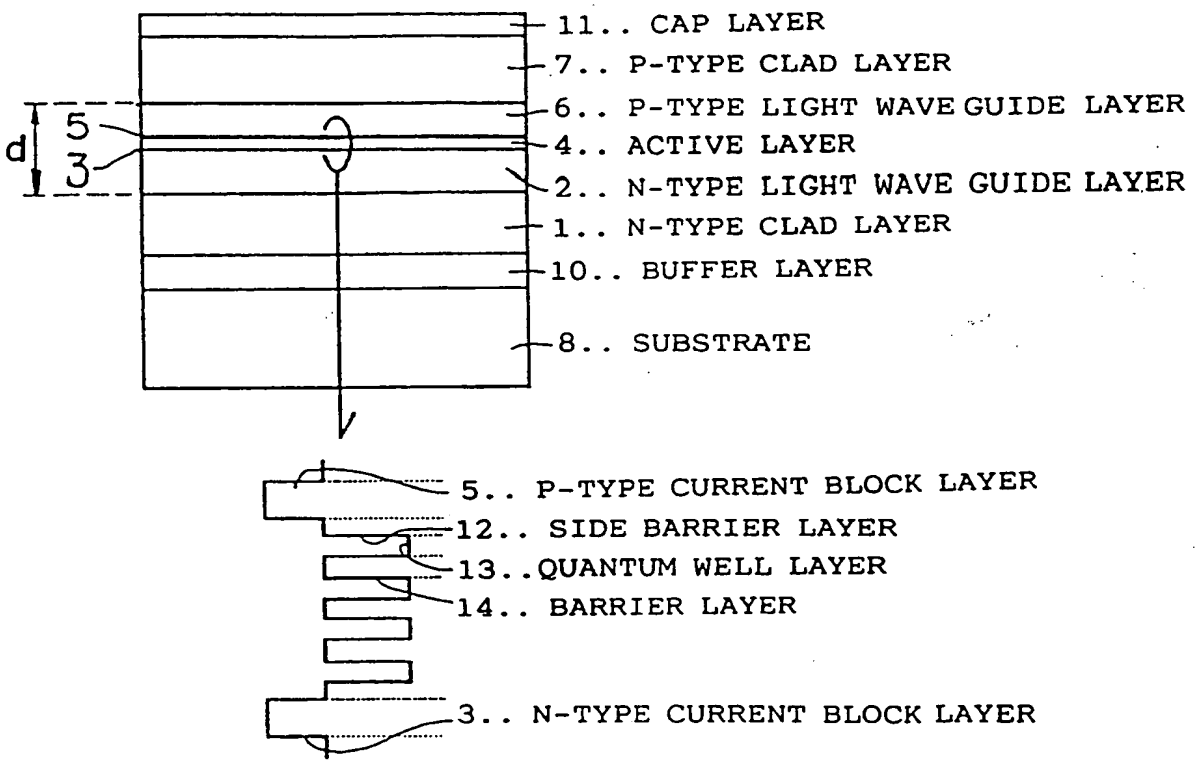


VIEW OF ACTIVE LAYER ENERGY BAND

FIG.15

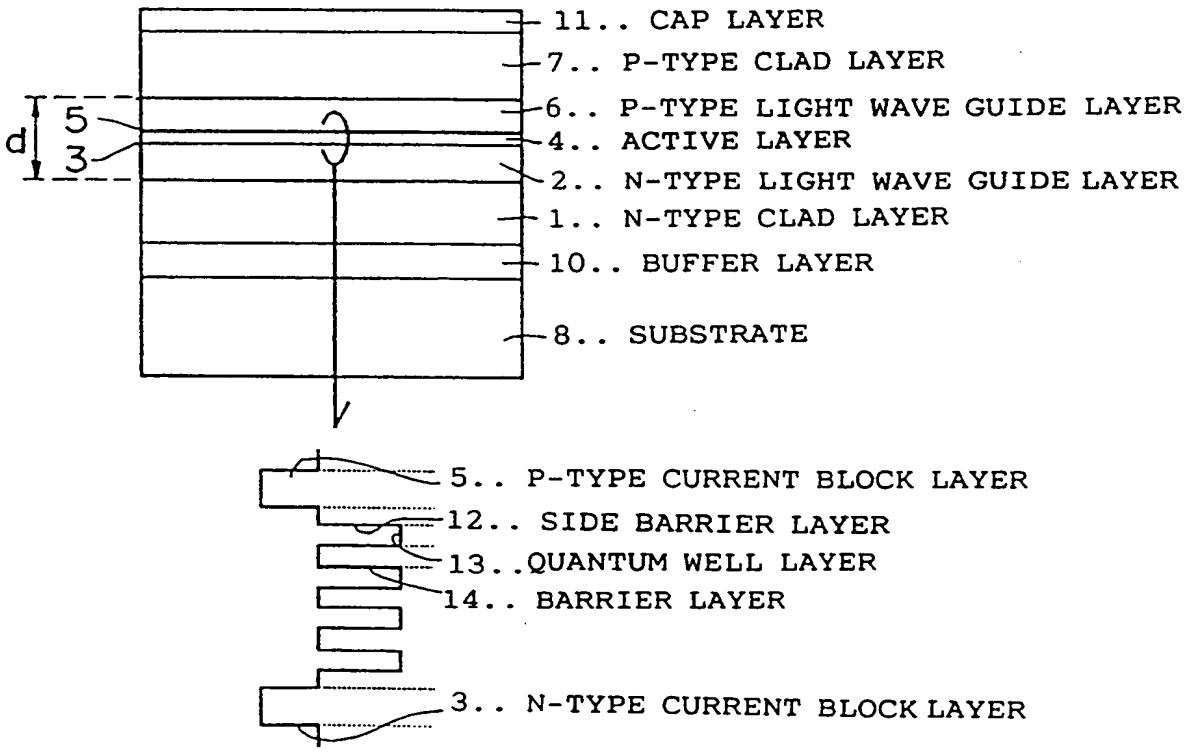


VIEW OF ACTIVE LAYER ENERGY BAND

FIG.16

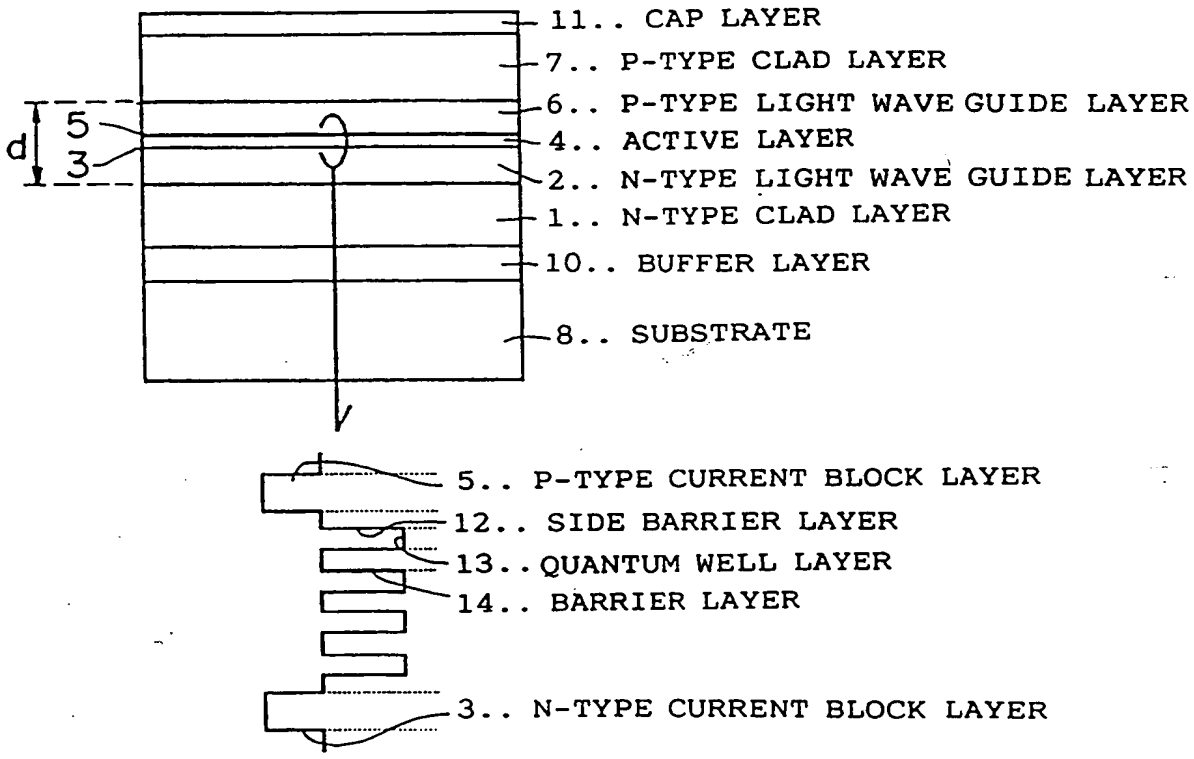


VIEW OF ACTIVE LAYER ENERGY BAND

FIG.17

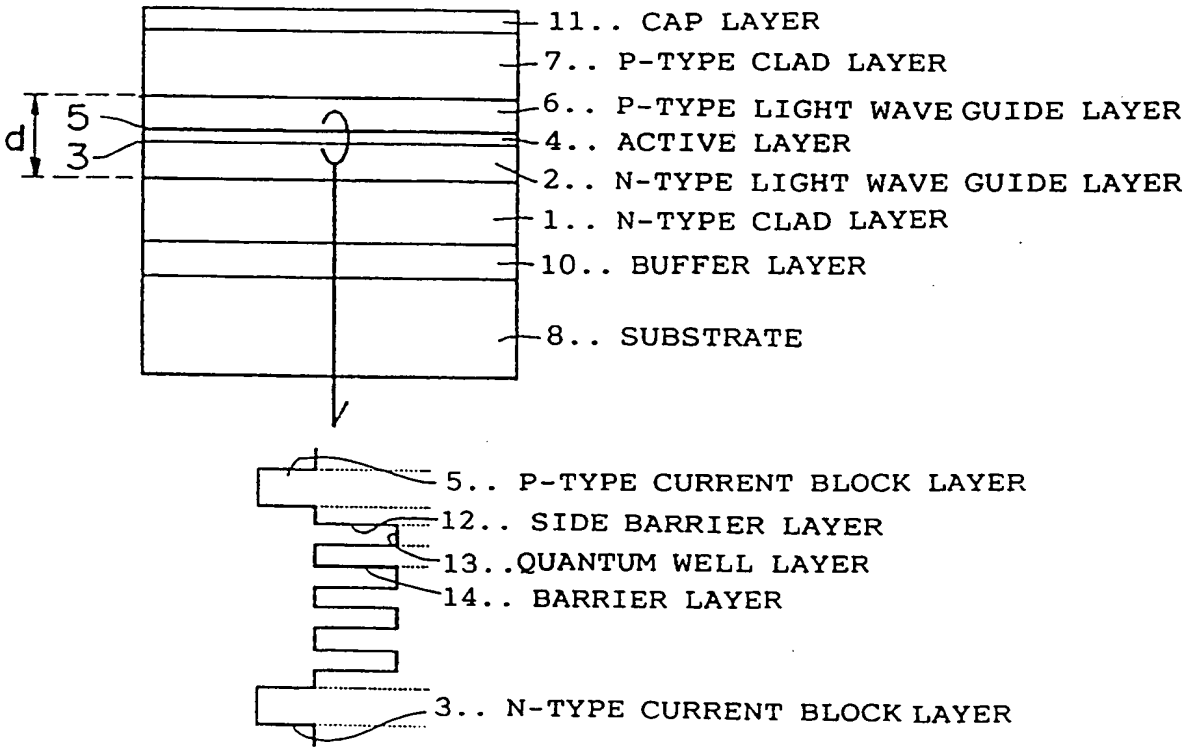


VIEW OF ACTIVE LAYER ENERGY BAND

FIG.18

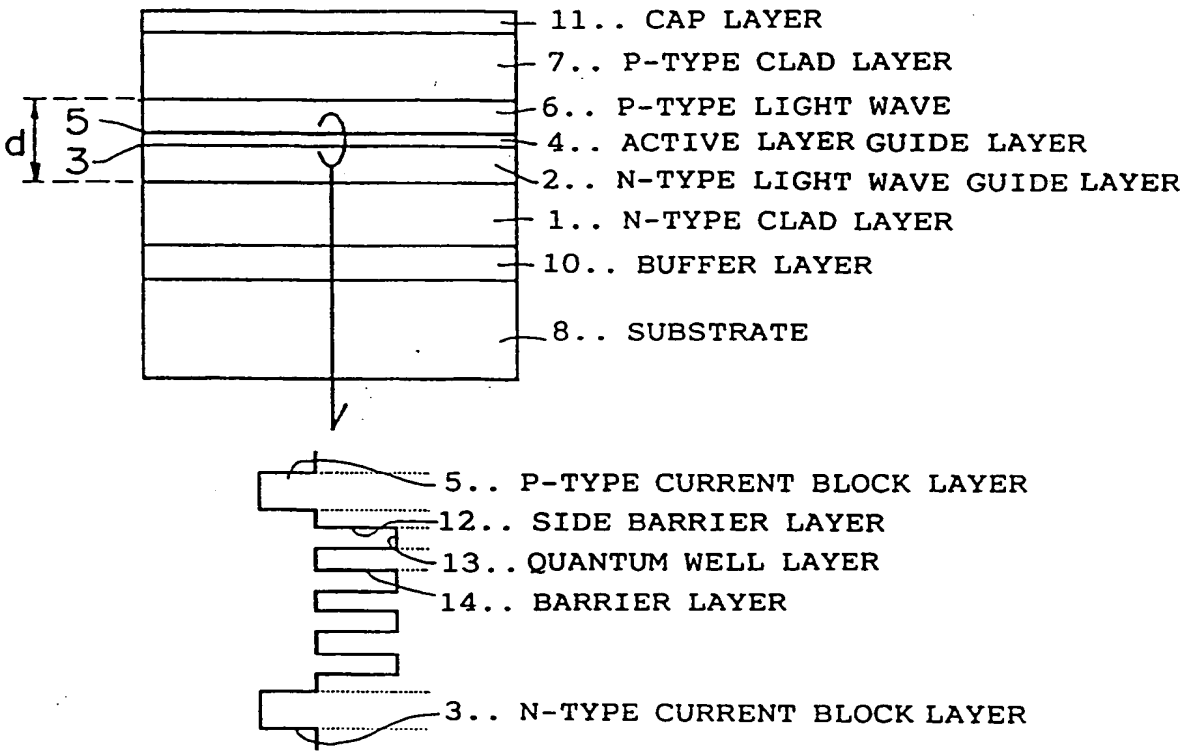


VIEW OF ACTIVE LAYER ENERGY BAND

FIG.19

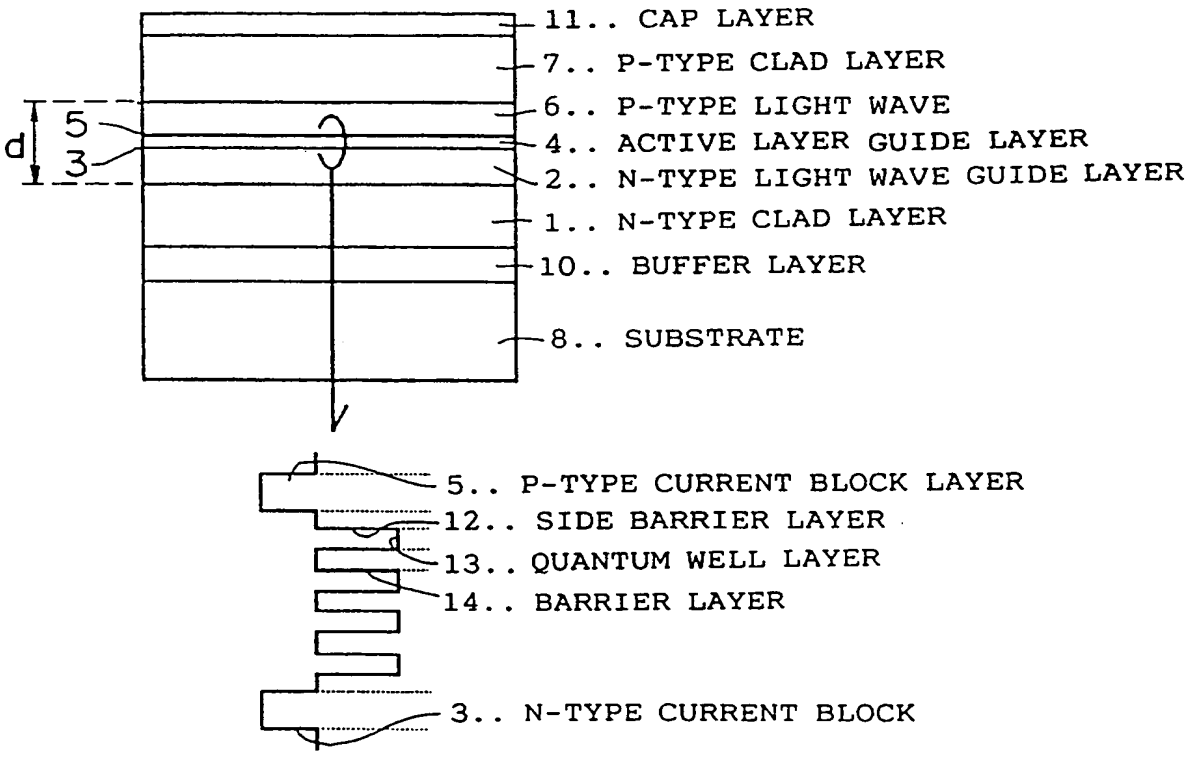


VIEW OF ACTIVE LAYER ENERGY BAND

FIG.20

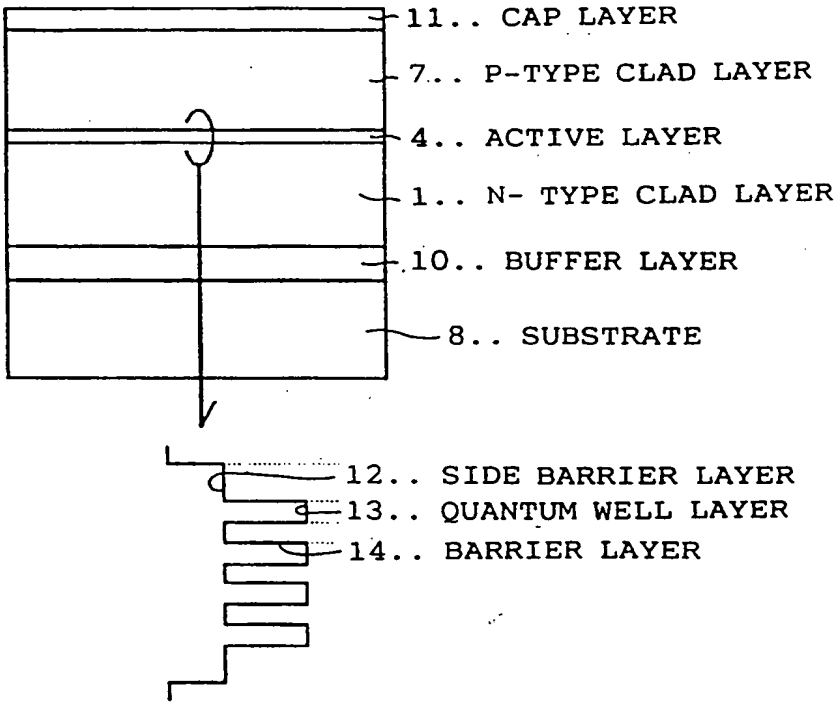


VIEW OF ACTIVE LAYER ENERGY BAND

FIG.21

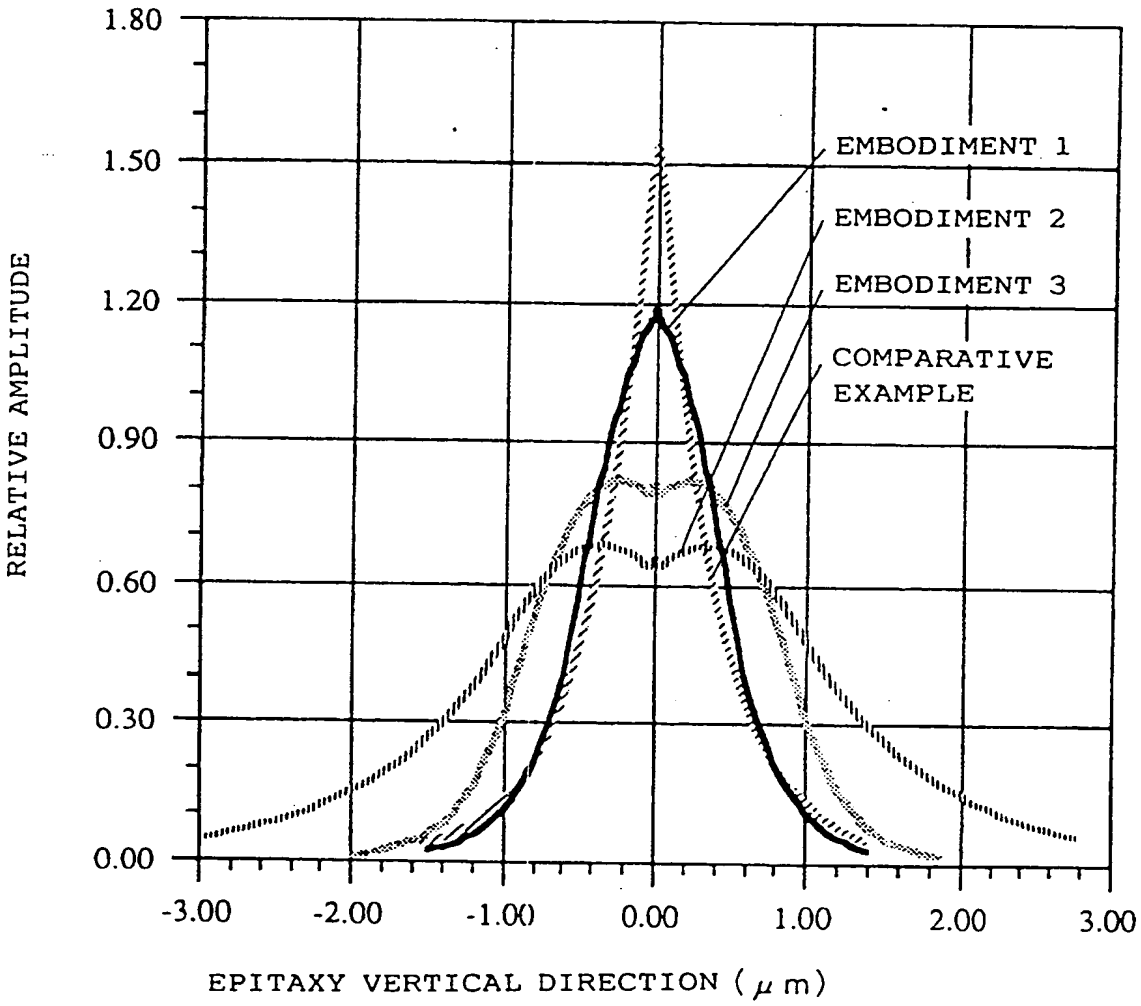


GUIDED MODE

FIG.22

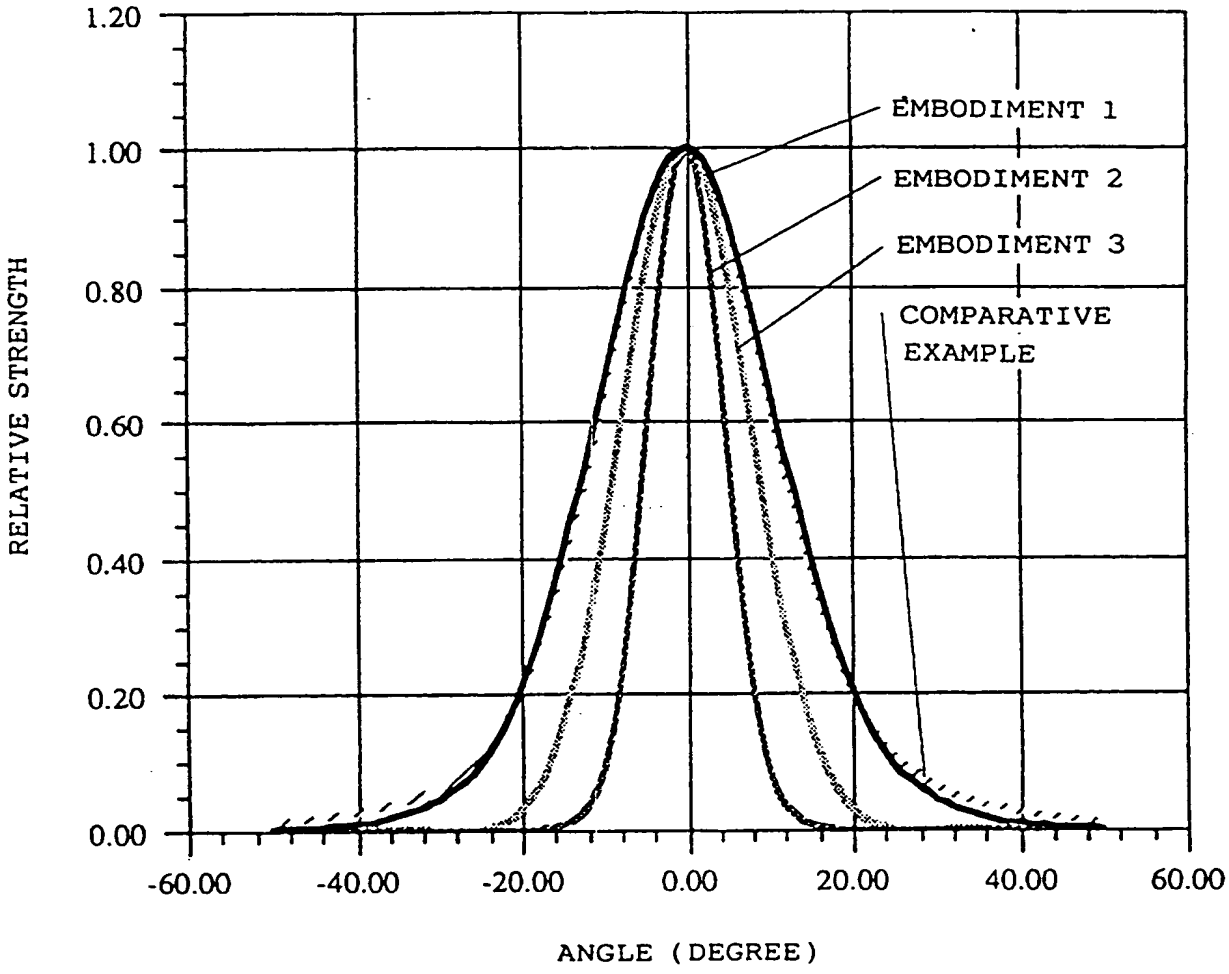


RADIATION MODE

FIG.23

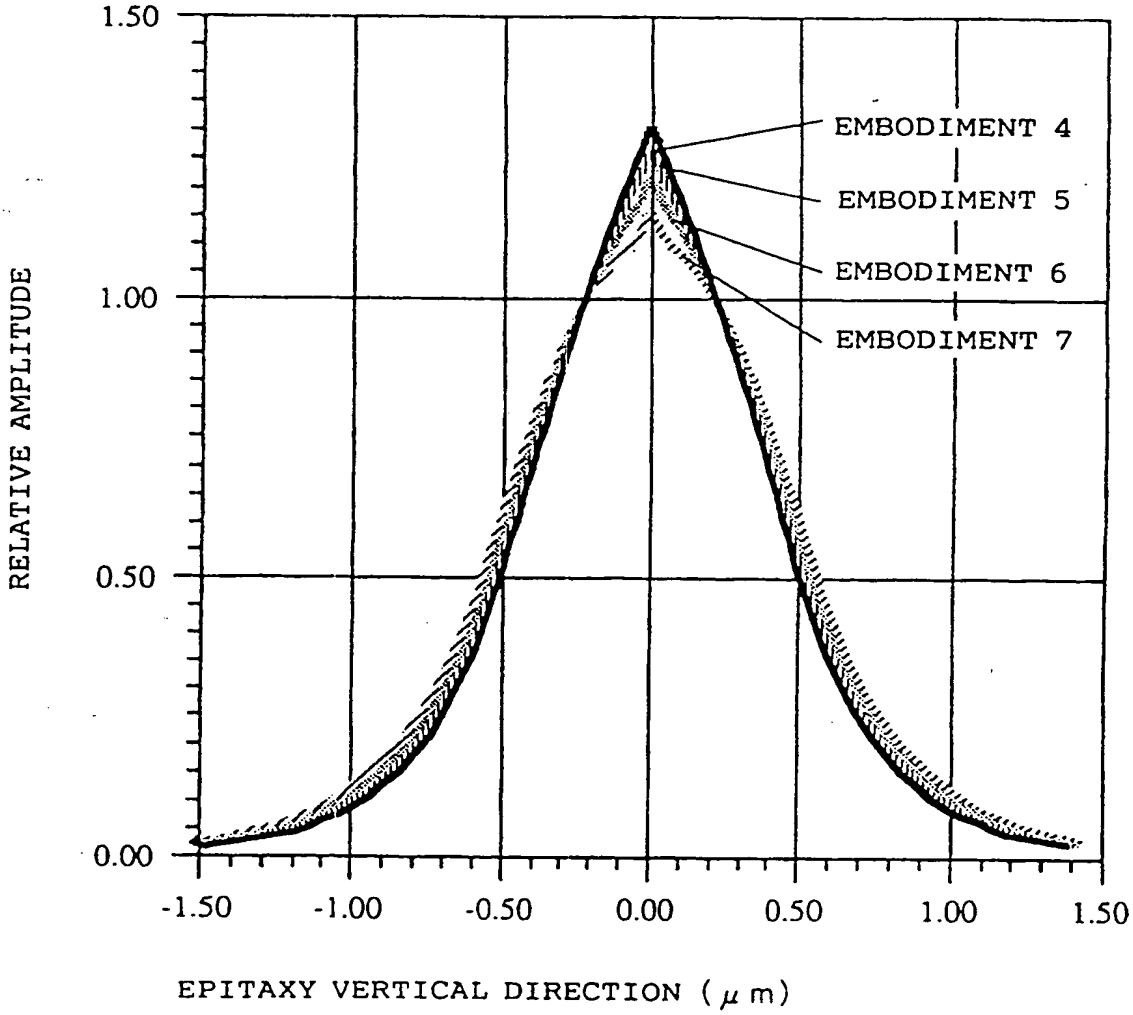


GUIDED MODE

FIG.24

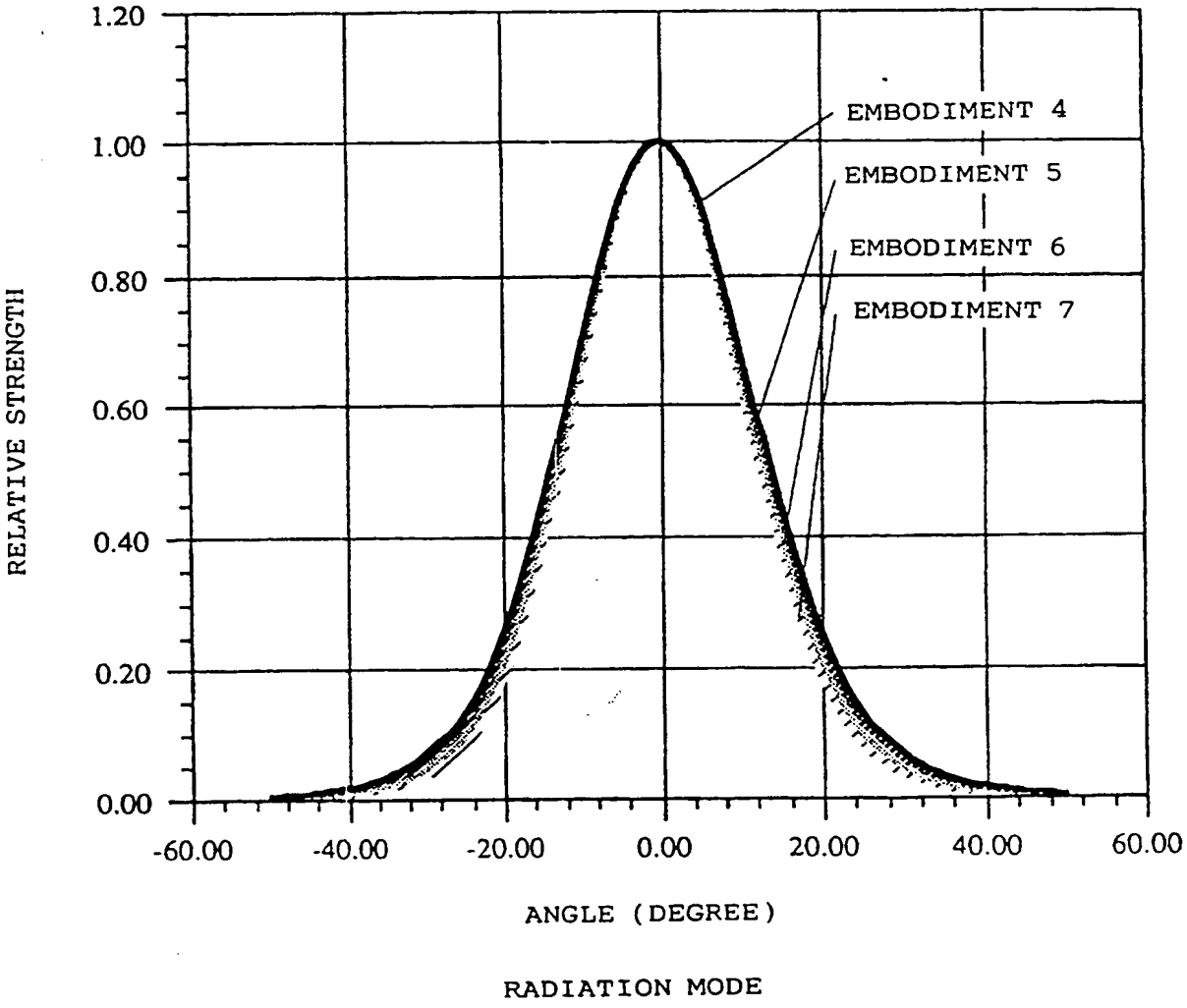


RADIATION MODE

FIG.25

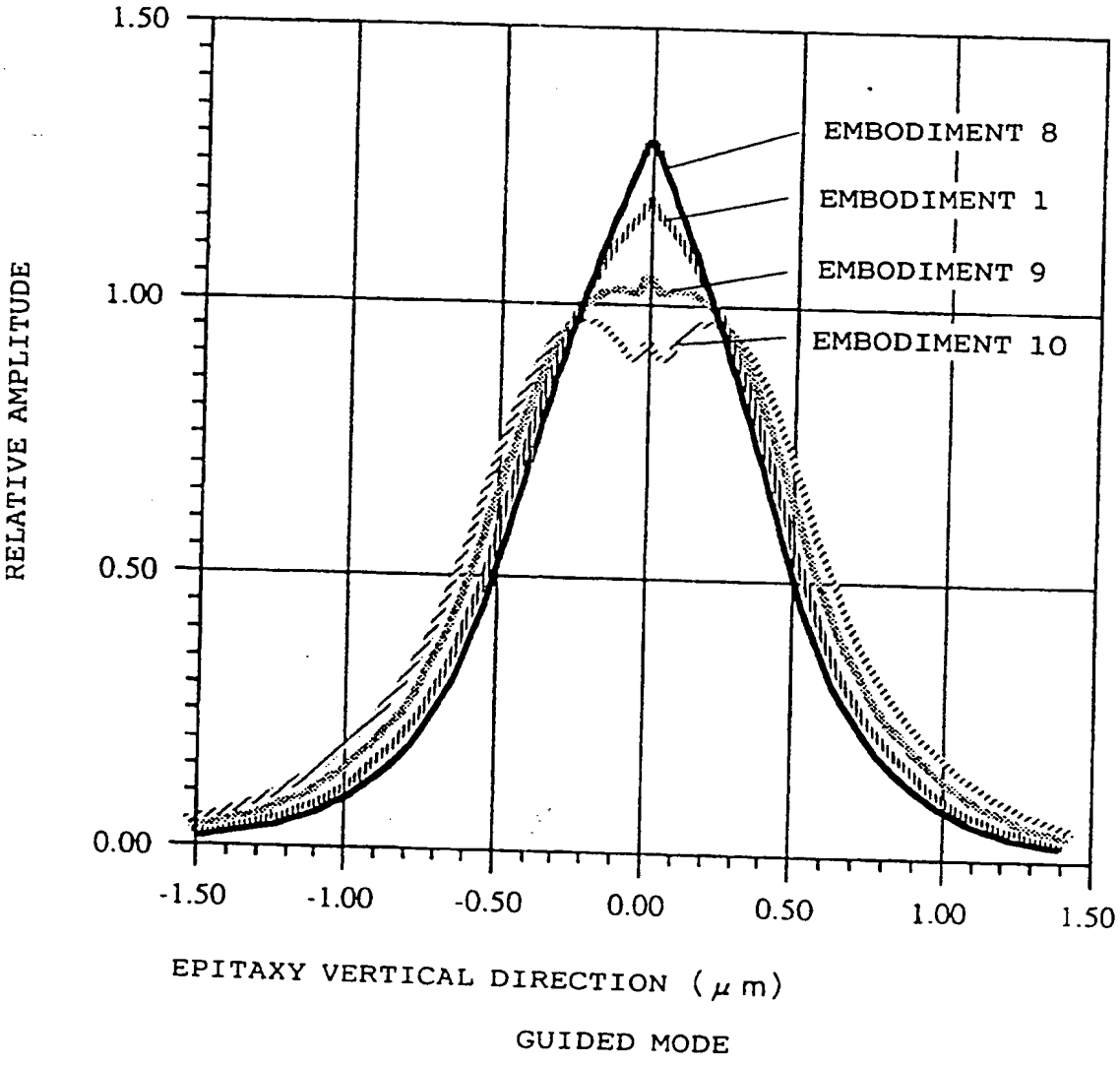
1.50
1.00
0.50
0.00
-1.50
-1.00
-0.50
0.00
0.50
1.00
1.50
RELATIVE AMPLITUDE
EMBODIMENT 8
EMBODIMENT 1
EMBODIMENT 9
EMBODIMENT 10
EPITAXY VERTICAL DIRECTION (μm)
GUIDED MODE

FIG.26

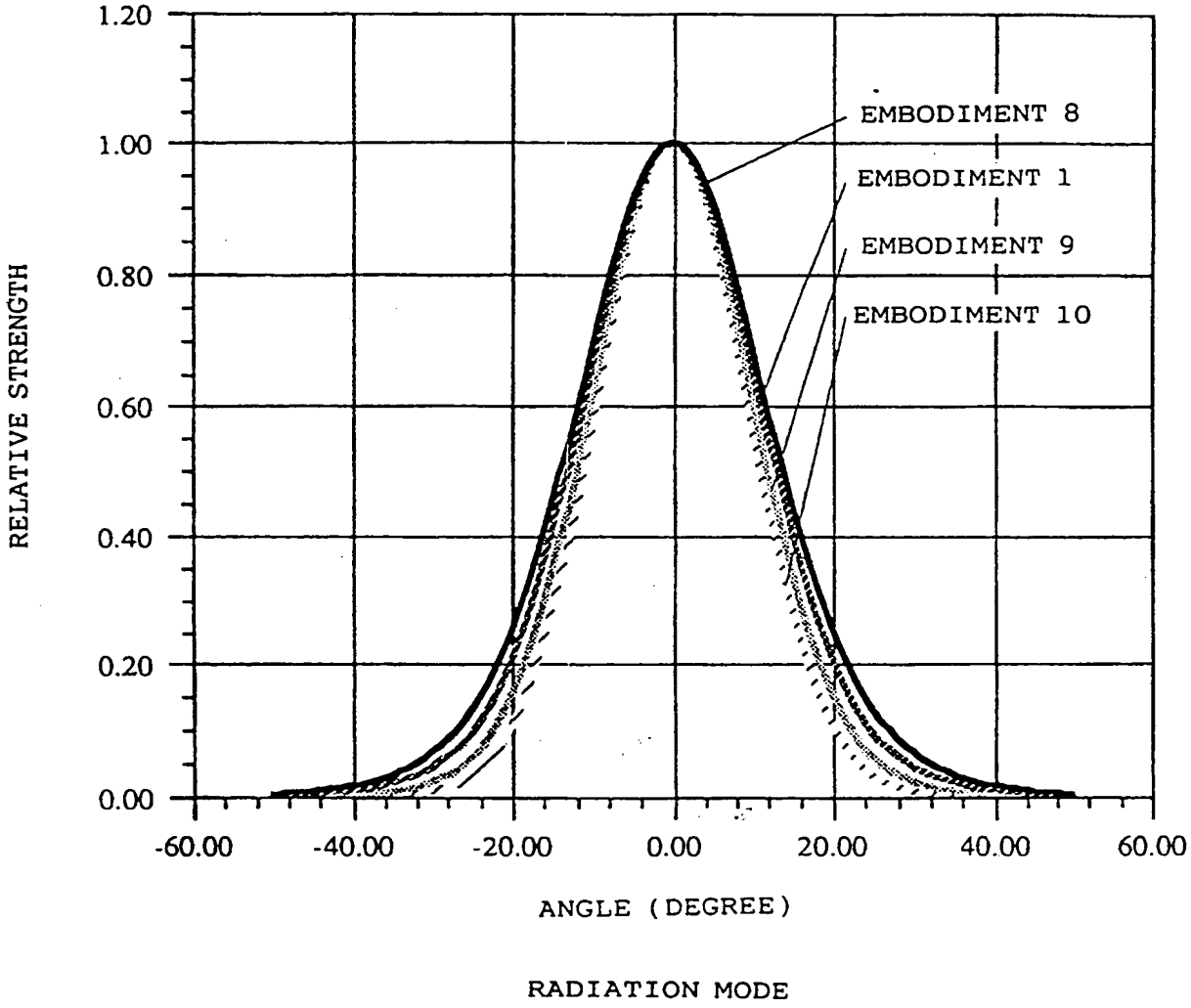
1.20
1.00
0.80
0.60
0.40
0.20
0.00
RELATIVE STRENGTH
EMBODIMENT 8
EMBODIMENT 1
EMBODIMENT 9
EMBODIMENT 10
-60.00
-40.00
-20.00
0.00
20.00
40.00
60.00
ANGLE (DEGREE)
RADIATION MODE

FIG. 27

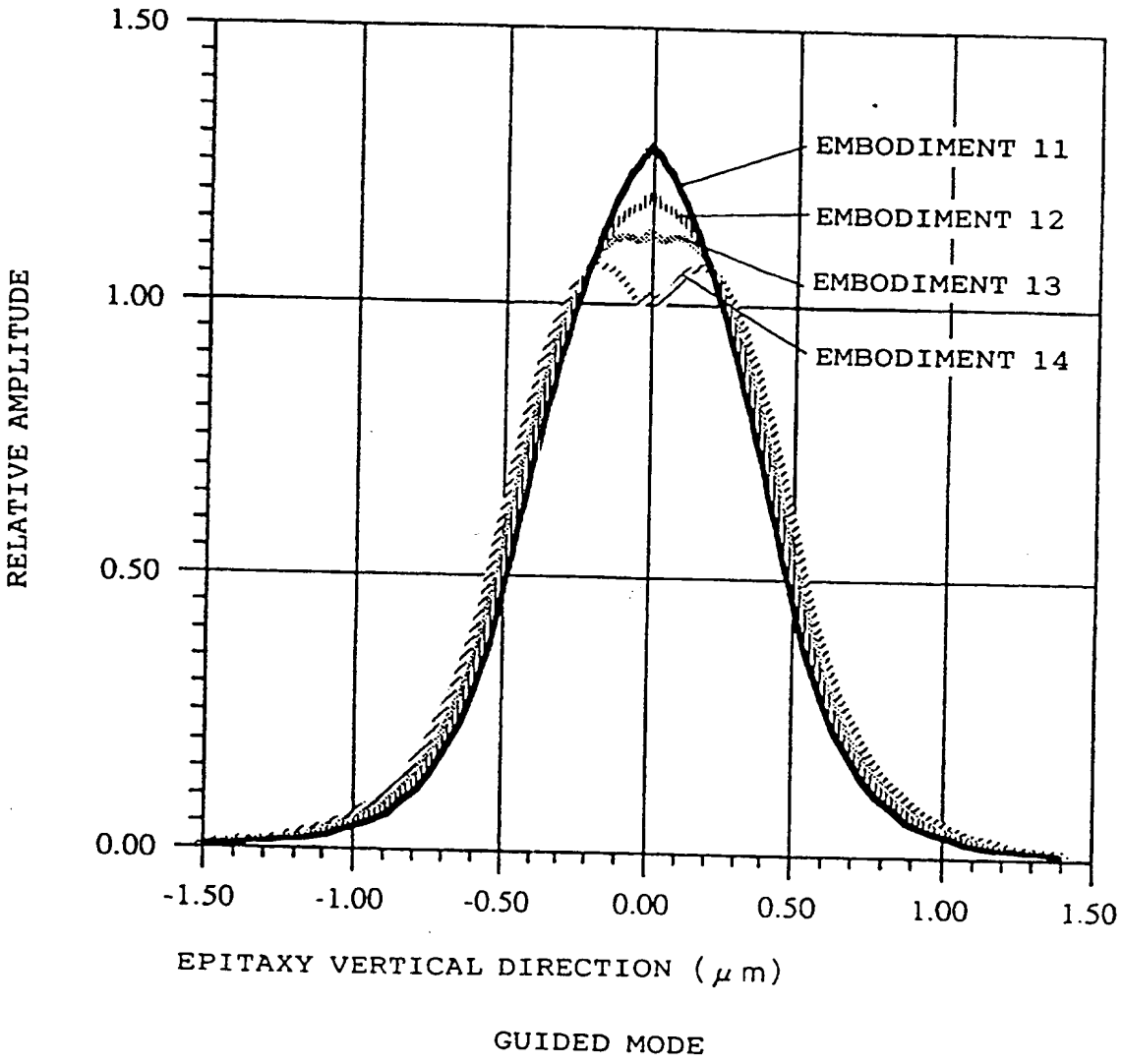
1.50
1.00
0.50
0.00
-1.50
-1.00
-0.50
0.00
0.50
1.00
1.50
RELATIVE AMPLITUDE
EPITAXY VERTICAL DIRECTION (μm)
EMBODIMENT 11
EMBODIMENT 12
EMBODIMENT 13
EMBODIMENT 14
GUIDED MODE

FIG.28

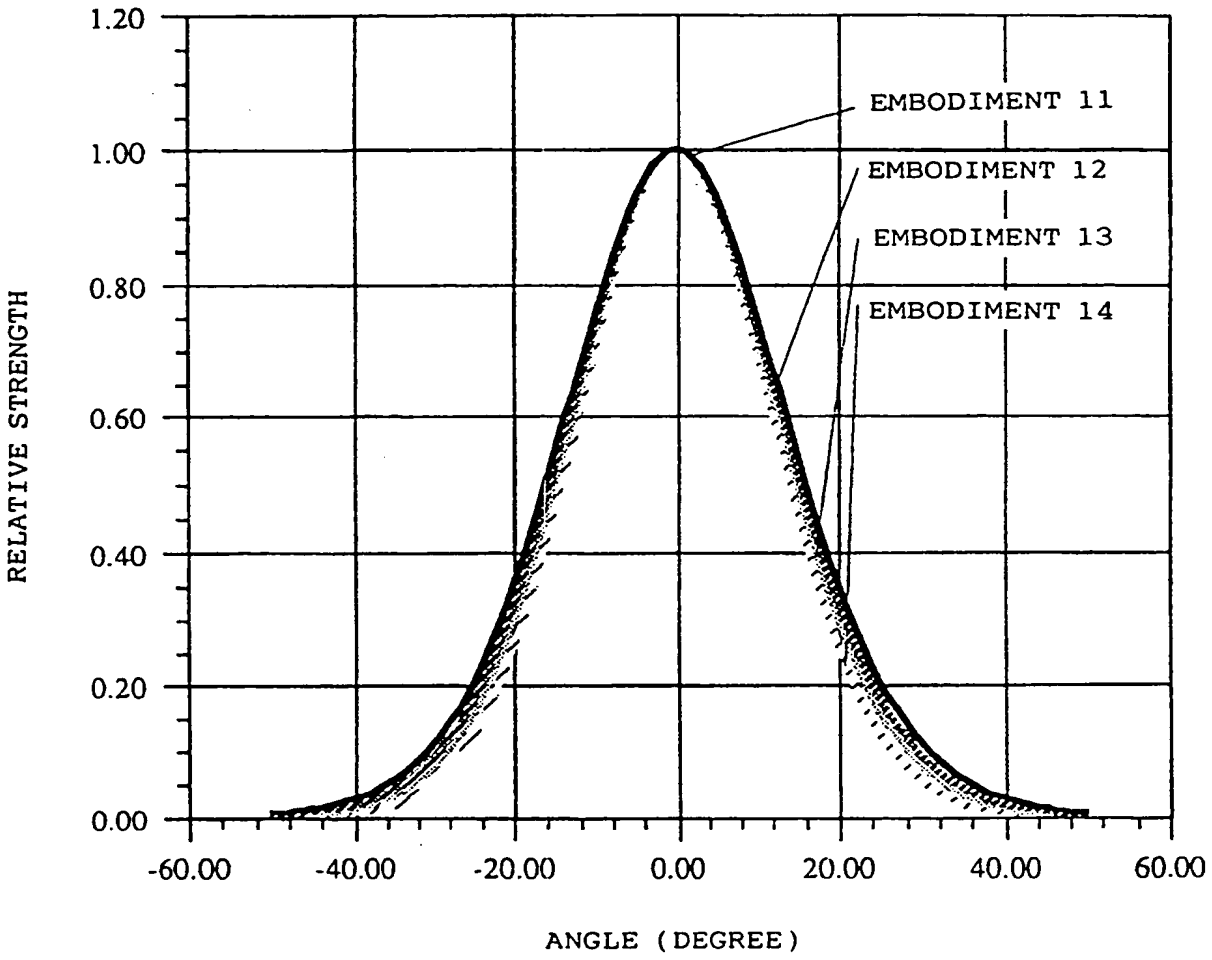


RADIATION MODE

FIG.29

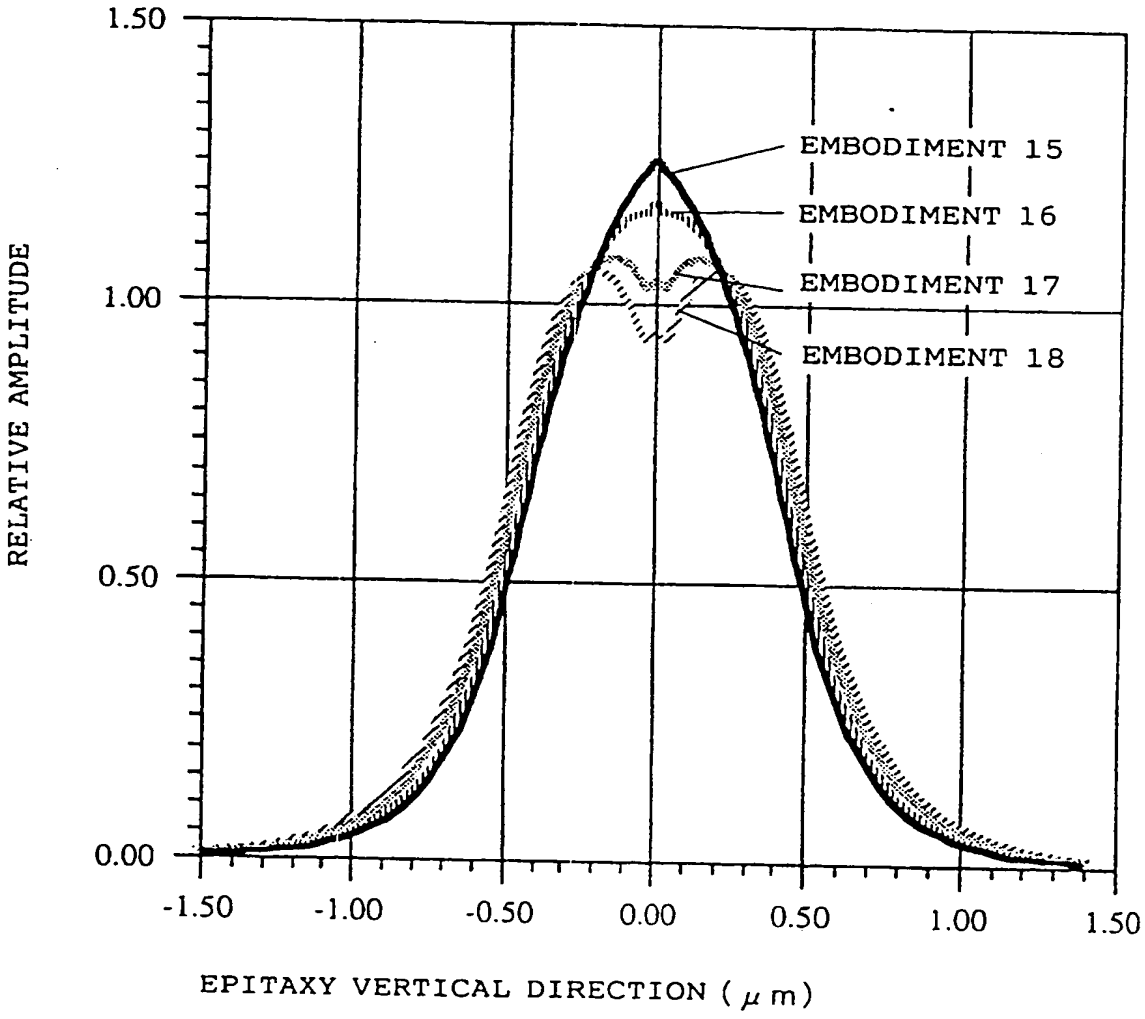
1.50
1.00
0.50
0.00
-1.50
-1.00
-0.50
0.00
0.50
1.00
1.50
RELATIVE AMPLITUDE
EMBODIMENT 15
EMBODIMENT 16
EMBODIMENT 17
EMBODIMENT 18
EPITAXY VERTICAL DIRECTION (μm)
GUIDED MODE

FIG.30

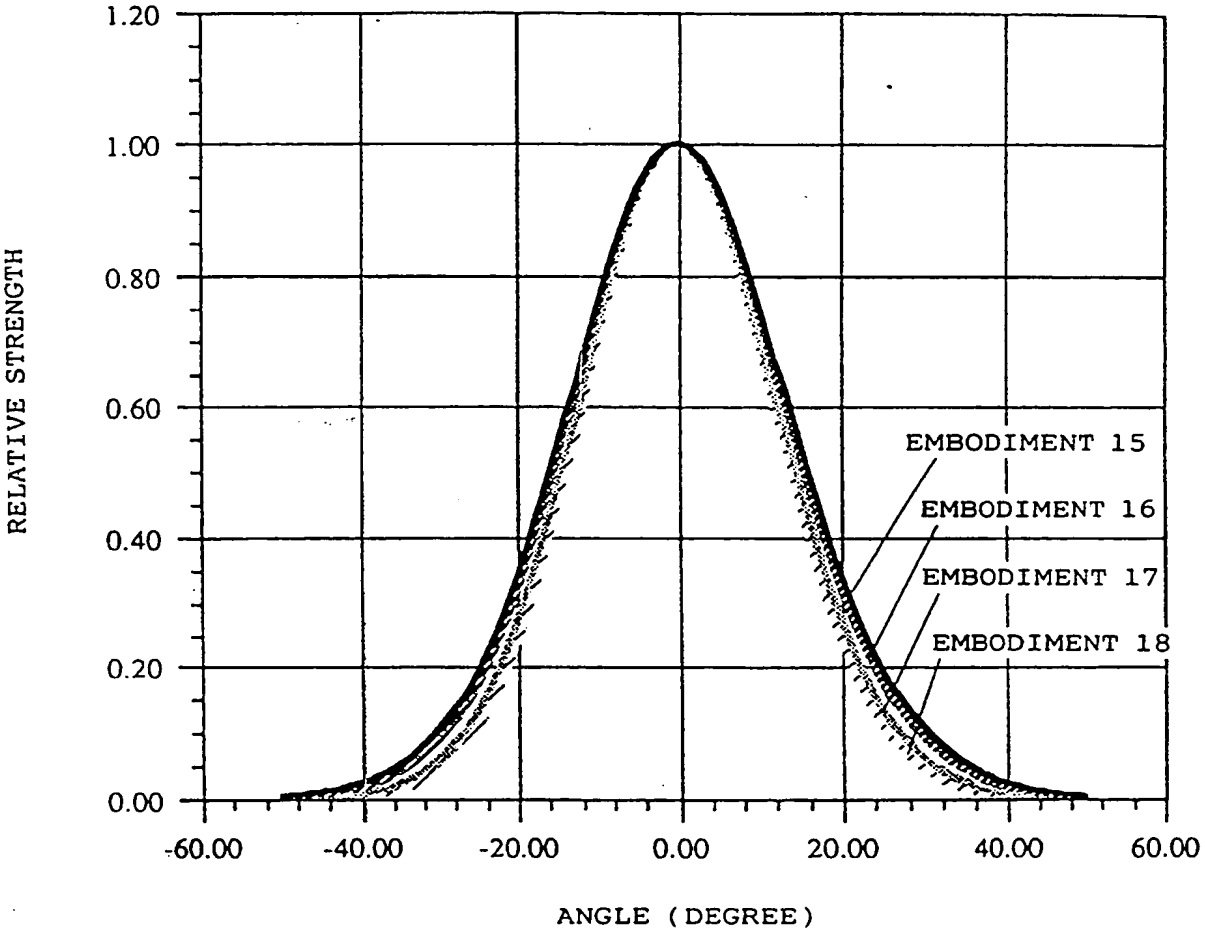


RADIATION MODE

FIG.31

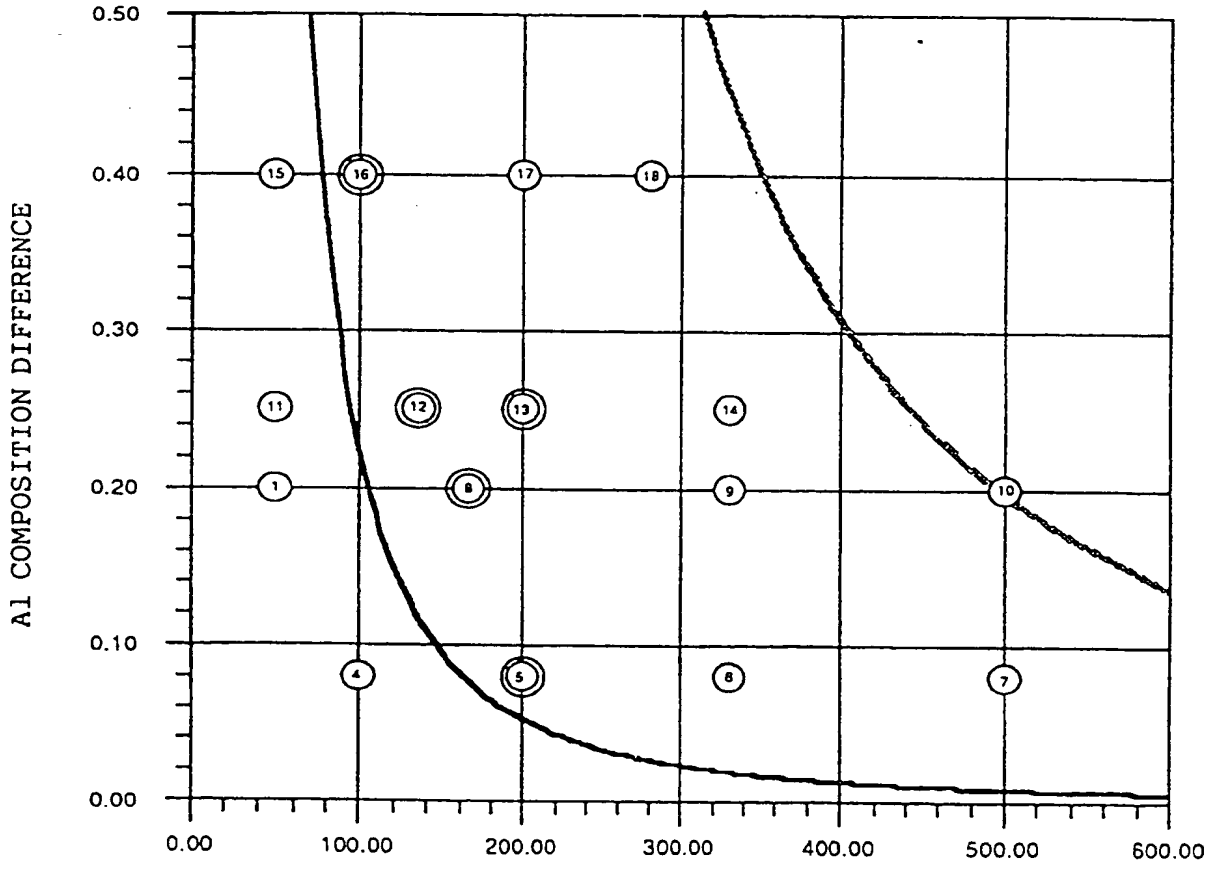
0.50
0.40
0.30
0.20
0.10
0.00
Al COMPOSITION DIFFERENCE
0.00
100.00
200.00
300.00
400.00
500.00
600.00
ANTI-GUIDING CARRIER BLOCK LAYER THICKNESS (Å)

FIG.32

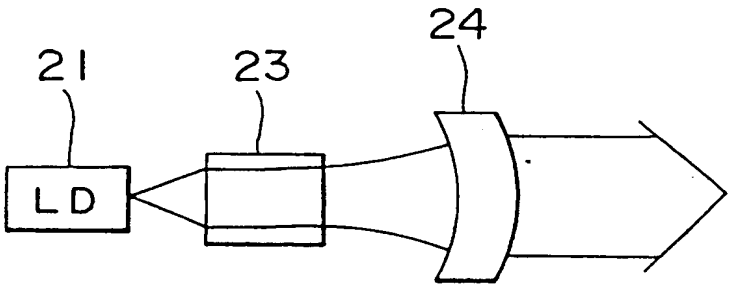


FIG.33

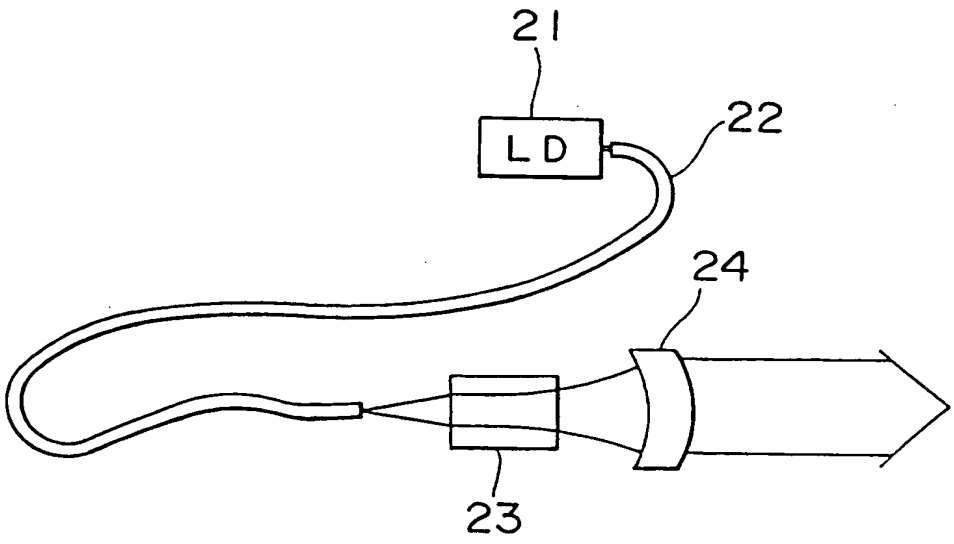

# INTERNATIONAL SEARCH REPORT

International application No.
PCT/JP93/00156

A. CLASSIFICATION OF SUBJECT MATTER

Int. Cl$^5$ H01S3/18, H01S3/094

According to International Patent Classification (IPC) or to both national classification and IPC

B. FIELDS SEARCHED

Minimum documentation searched (classification system followed by classification symbols)

Int. Cl$^5$ H01S3/18, H01S3/094

Documentation searched other than minimum documentation to the extent that such documents are included in the fields searched

Jitsuyo Shinan Koho 1964 - 1992
Kokai Jitsuyo Shinan Koho 1973 - 1992

Electronic data base consulted during the international search (name of data base and, where practicable, search terms used)

C. DOCUMENTS CONSIDERED TO BE RELEVANT

| Category* | Citation of document, with indication, where appropriate, of the relevant passages | Relevant to claim No. |
|---|---|---|
| X<br>X | JP, A, 61-15385 (NEC Corp.),<br>January 23, 1986 (23. 01. 86),<br>Figs. 1, 2<br>Line 1, lower left column to<br>line 1, lower right column, page 2<br>(Family: none) | 1<br>5 |
| X<br>Y | JP, A, 60-133781 (NEC Corp.),<br>July 16, 1985 (16. 07. 85),<br>Figs. 1, 2<br>Lines 3 to 5, upper left column, page 3<br>(Family: none) | 1-2<br>7 |
| X | JP, A, 2-150087 (Asahi Glass Co., Ltd.),<br>June 8, 1990 (08. 06. 90),<br>Fig. 1 (Family: none) | 8-10 |

[X] Further documents are listed in the continuation of Box C. [ ] See patent family annex.

* Special categories of cited documents:
"A" document defining the general state of the art which is not considered to be of particular relevance
"E" earlier document but published on or after the international filing date
"L" document which may throw doubts on priority claim(s) or which is cited to establish the publication date of another citation or other special reason (as specified)
"O" document referring to an oral disclosure, use, exhibition or other means
"P" document published prior to the international filing date but later than the priority date claimed
"T" later document published after the international filing date or priority date and not in conflict with the application but cited to understand the principle or theory underlying the invention
"X" document of particular relevance; the claimed invention cannot be considered novel or cannot be considered to involve an inventive step when the document is taken alone
"Y" document of particular relevance; the claimed invention cannot be considered to involve an inventive step when the document is combined with one or more other such documents, such combination being obvious to a person skilled in the art
"&" document member of the same patent family

| Date of the actual completion of the international search | Date of mailing of the international search report |
|---|---|
| April 2, 1993 (02. 04. 93) | April 27, 1993 (27. 04. 93) |
| Name and mailing address of the ISA/<br>Japanese Patent Office<br>Facsimile No. | Authorized officer<br><br>Telephone No. |

Form PCT/ISA/210 (second sheet) (July 1992)